CURJ

WINTER 2011–12 vol. 12, no. 1

CALTECH UNDERGRADUATE RESEARCH JOURNAL

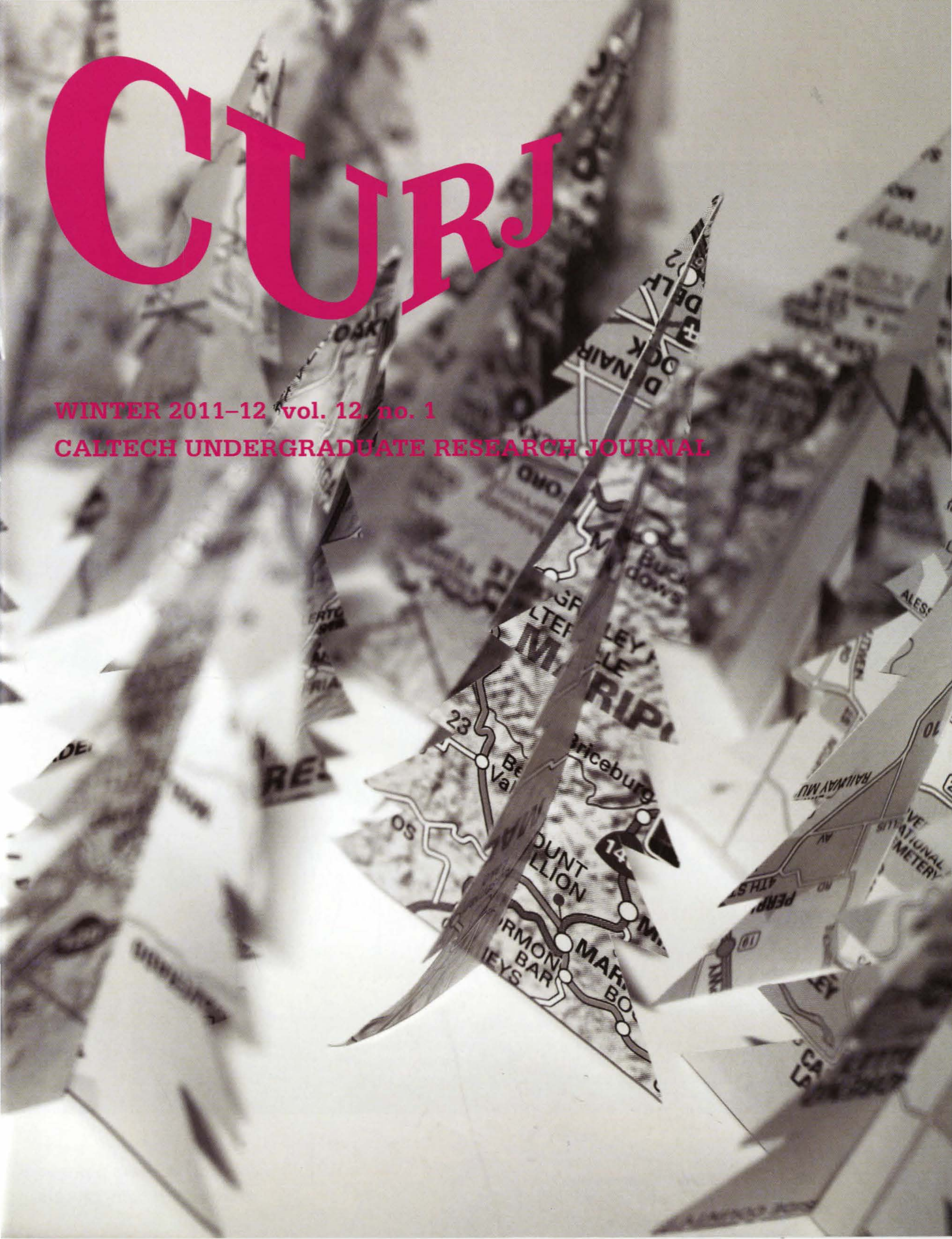

Lam
RESEARCH

Take Your Career to the Next Level

Lam Research Corporation is a leading supplier of wafer fabrication equipment and services to the worldwide semiconductor industry, where we have been advancing semiconductor manufacturing for over 30 years.

The Company has been number one in plasma etch market share for 10 consecutive years and maintains one of the largest installed bases of single-wafer wet clean modules.

With corporate headquarters located in Fremont, California, the company maintains a network of facilities throughout North America, Europe, and Asia. Our values-based culture creates a fast-paced environment that fosters creativity, offers opportunity, and recognizes and rewards achievement.

Lam Research – a company where successful people want to work

Lam Research has programs that allow students to continue their career development and build on their educational accomplishments.

Our new college graduates and interns work closely with some of the most talented people in the industry.

We combine educational training with hands-on experience to deliver new technologies and services that ensure our customers' success.

Lam Research looks for interns, new college graduates, individuals with MBAs, advanced degrees, and post-doctorates. We also have opportunities for experienced professionals.

New College Graduates

Lam Research offers new college graduates opportunities to play key roles in bringing innovative technology and business solutions to market in countries around the world.

College Internships

Lam's internship opportunities offer summer and/or co-op employment for students and provide hands-on business experience that complements academic studies.

Degree levels:

- *Ph.D.*
- *MBA*
- *Master's*
- *Bachelor's*

Areas of discipline:

- *Chemistry*
- *Engineering (Chemical, Computer, Electrical, Industrial, Manufacturing, and Mechanical)*
- *Field Service Operations*
- *Finance*
- *Human Resources*
- *Information Systems*
- *Management Information Systems*
- *Marketing*
- *Materials Science*
- *Physics*
- *Plasma Physics*
- *Research & Development*
- *Software Development*
- *Supply Chain*

Contact Remiel Woo-Chamberlain at remiel.woo-chamberlain@lamresearch.com about Lam Research opportunities.

visit our careers page at lamresearch.com/careers

INTERVIEW

RESEARCH

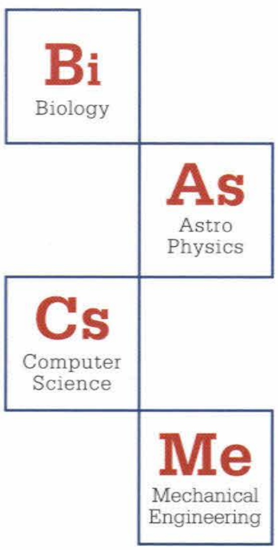

CALTECH UNDERGRADUATE
RESEARCH JOURNAL VOL. 12 NO. 1

LETTER FROM THE EDITORS

Caltech, a prominent institution at the forefront of scientific discovery, houses some of the best and brightest students in the world. With only about 300 professional faculty, Caltech hosts an undergraduate student body just barely under 1000 students and a graduate student body of about 1200 students. At such low numbers, Caltech has, time and time again, been able to produce some of the world's best innovations.

However, doing the research is only half the battle. Almost as difficult as the research, communication is a real issue in today's scientific media outreach. What use is research without communication with other scientists, students, and the public? The best way to move forward is to facilitate collaboration and cultivate a sense of urgency and unity towards a common goal: improving and educating the world through scientific knowledge.

The Caltech Undergraduate Research Journal aims to showcase the talent of young scientists at Caltech, while also providing them with an opportunity to perform scientific writing and an introduction into the publishing process. Unfortunately, the Caltech Undergraduate Research Journal can only highlight a small fraction of the great research done at Caltech. All the students at Caltech deserve recognition for their dedication and commitment to science.

Of course, the student research at Caltech could not have been completed without the support of dedicated faculty and mentors. Because of the great faculty, the Caltech Undergraduate Research Journal is proud to highlight a distinguished faculty member at Caltech, professor Jacqueline Barton.

Jacqueline Barton is distinguished for her research on DNA and long-range electron transfer, earning the nation's top science award, the National Medal of Science. She has undoubtedly made landmark contributions in the scientific community. Caltech would certainly not be as outstanding without her and other faculty.

We thank you for picking up the latest edition of CURJ and hope that you may take the time to learn about some of the people and research at Caltech. Inside this issue is the research of four undergraduate researchers who covered topics from elucidating the mechanism of pulmonary hypertension to locating binary systems of white dwarfs. As always, feel free to look at past issues of the Caltech Undergraduate Research Journal and find more content on our website (curj.caltech.edu).

Best regards,

Granton Jindal and Marvin Gee

Zhaoying Xian

Mentors:
Marlene Rabinovitch
Christopher Rhodes

Extracellular Sulfatase-2 Levels in Idiopathic Pulmonary Arterial Hypertension

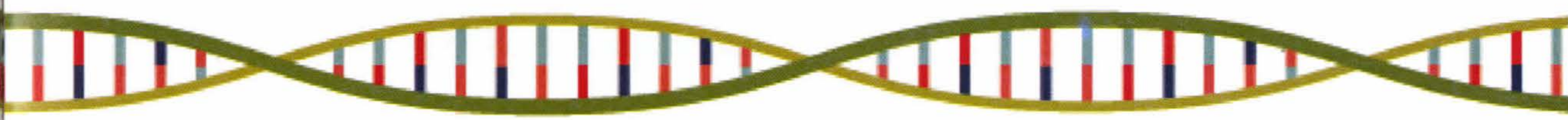

Idiopathic pulmonary arterial hypertension (IPAH) is a rare and incurable disease. As a type of pulmonary hypertension, it is characterized by increased blood pressure in the arteries of the lungs, which forces the right side of the heart to work harder to pump blood against the increased pressure. IPAH often results in heart failure and death; the average prognosis of IPAH patients is only 2.8 years without treatment. The disease is not well understood, but endothelial dysfunction seems to be pivotal to the pathological changes associated with IPAH. Thus, in order to better understand the mechanisms of IPAH, this research focuses on studying changes in gene expression in cultured pulmonary artery endothelial cells.

BACKGROUND

IPAH is not well understood, but current research suggests genetic factors. Researchers have observed a mutation in bone morphogenetic protein receptor (BMPRII) in a large proportion of IPAH patients, as well as overall decreased expression of BMPRII in all IPAH patients. Other mutations in members of the TGF-β signaling pathway have been identified, but only vary rarely in patients with IPAH.

Interestingly, IPAH is more prevalent in females, by a factor of 2. In general, IPAH displays pathological features associated with endothelial dysfunction such as loss of pre-capillary microvessels through apoptosis, and reduced production of endothelial cell (EC) factors such as nitric oxide and apelin that inhibit proliferation of the smooth muscle cells (SMC).

Current treatments are symptomatic; to discover more effective remedies, it is imperative to understand the mechanisms of IPAH.

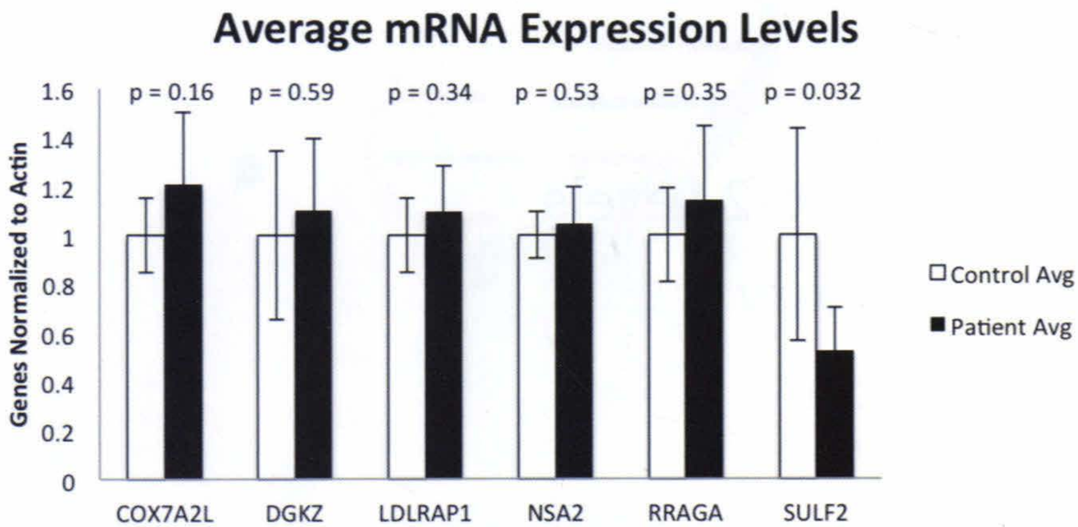

Figure 1 – Quantitative RT-PCR analysis of gene expression in control and IPAH PAECs.
The above graph summarizes the results of qRT-PCR analysis of the 6 genes of interest identified by RNA-seq in 6 versus 6 control and IPAH PAEC cell lines. Bars indicate standard error and statistics shown are for t-tests. The genes tested for mRNA expression are cytochrome c oxidase VIIa related protein (COX7A2L), diacyl glycerol kinase zeta (DGKZ), low-density lipoprotein receptor adapter protein 1 (LDLRAP1), TGF-β (transforming growth factor beta) inducible nuclear protein (NSA2), ras-related GTP binding protein A (RRAGA), and extracellular sulfatase 2 (SULF2).

The disease is not well understood, but endothelial dysfunction seems to be pivotal to the pathological changes.

SULF2 IS DIFFERENTIALLY EXPRESSED

This project focused on studying changes in gene expression in cultured pulmonary artery endothelial cells (PAECs) that were identified by RNA-seq. RNA-seq is a technique that involves sequencing cDNA produced from RNA in order to obtain sequencing as well as RNA expression data. The PAECs were harvested from 3 unused donor lungs and 3 patients with IPAH. Thus, to find changes in PAEC gene expression, we compared the mRNA isoform transcript levels in the control and IPAH PAECs.

Twenty-four genes were identified to be either up or down regulated in the IPAH vs. control PAECs. Of those twenty-four, six genes of interest with obvious relevance to IPAH were selected for further study. Quantitative real-time PCR (qRT-PCR), a technique that quantifies the amount of cDNA in a sample, was used to compare mRNA expression levels of the 6 target genes. Only SULF2 showed consistently significant and differential levels of mRNA expression after normalization to a housekeeping gene, β-actin. (Figure 1). In the IPAH cells lines, SULF2 mRNA levels were significantly lower (p=0.032).

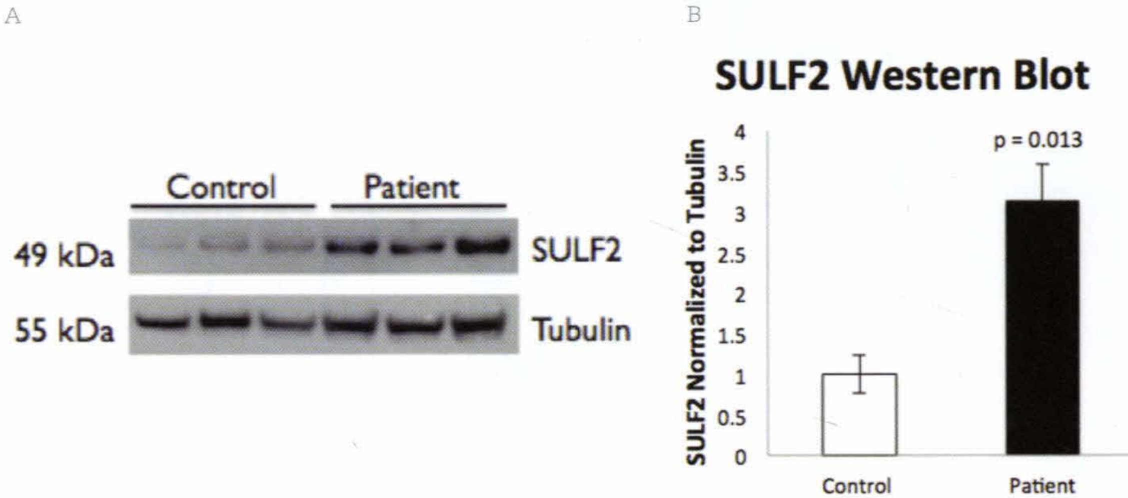

Figure 2 – Western blot analysis of SULF2 protein expression in control and IPAH PAECs.
(a) Western blot analysis of SULF2 in 3 vs. 3 control and IPAH PAEC cell lines. Tubulin was used as a loading control. The intensity of each signal is directly related to the level of protein expression. (b) The graph shows densitometry analysis of the western blot, with bars indicating standard error and the t-test p-value shown.

Current treatments are symptomatic; to discover more effective remedies, it is imperative to understand the mechanisms of IPAH.

Next, the protein levels of SULF2 were analyzed using western blotting. The results of the western blot were normalized to the loading control tubulin (Figure 2). SULF2 protein was differentially expressed between the patient and control PAECs ($p = 0.013$). Interestingly, in contrast to the reduced levels of mRNA, the protein level was significantly increased in the patient PAECs.

Finally, we studied localization of SULF2 using immunofluorescence. Cells were stained in normal culture conditions and after permeabilisation to assess extracellular and intracellular localization. No staining was observed on the non-permeable control cells. The non-permeable patient cells appear to show primarily nuclear staining, with minimal extracellular or cytosolic staining. SULF2 was observed only in the nucleus for both the permeable control and patient cells, which is unexpected since previous research has shown that it is an extracellular protein. (Figure 3)

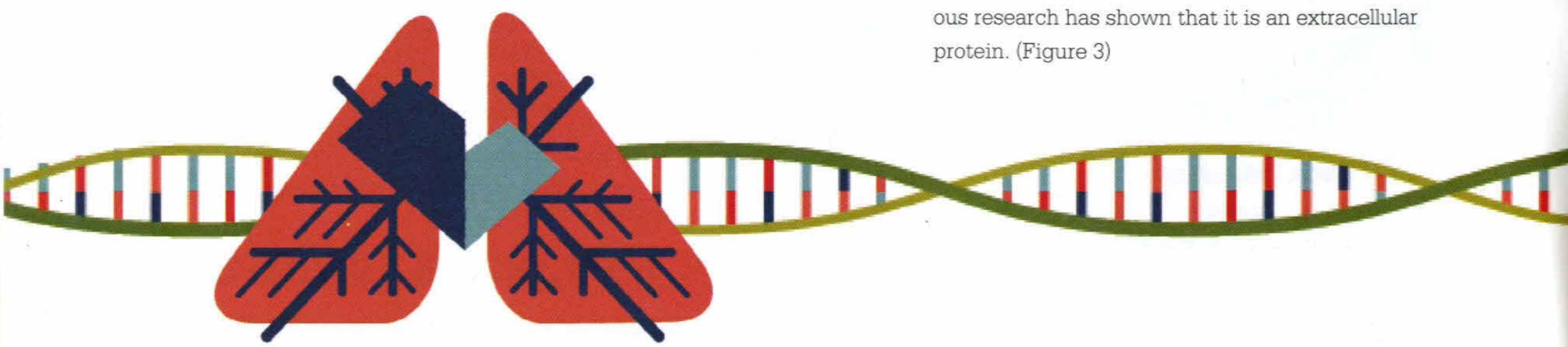

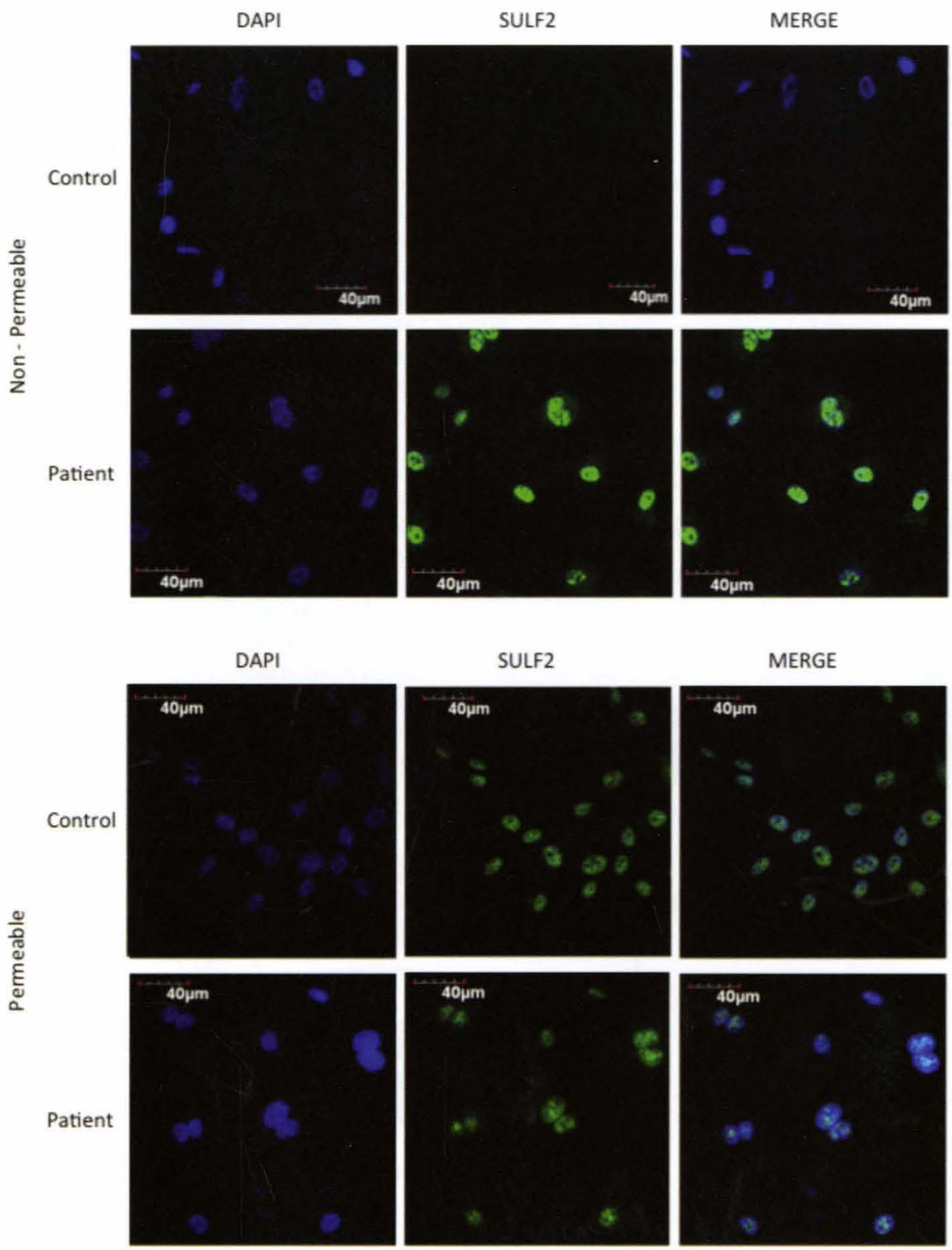

Figure 3 – SULF2 immunofluorescence in control and patient PAECs, with and without permeabilisation. DAPI (blue) indicates cell nuclei. SULF2 is stained in green. The images shown are representative of all the images taken.

SULF2's POSSIBLE ROLES IN IPAH

Extracellular sulfatase 2 (SULF2) is an extracellular protein highly expressed in many organs and tissue, such as the heart. SULF2 regulates heparan sulfate proteoglycans (HSPG) (Figure 4). HSPGs are located on the surface of cells and bind growth factors such as Wingless (Wnt) or fibroblast growth factors (FGFs) to inhibit them from activating their downstream receptors. SULF2 selectively removes 6-O-sulfate groups from the HSPGs. This facilitates the release of previously bound growth factors, which then activate their receptors. This can lead to the activation of downstream signaling cascades such as the Wnt signaling pathway. Therefore, altered SULF2 activity in IPAH could lead to downstream effects on both cell proliferation and survival.

Since SULF2 is an extracellular protein, it could have effects on other cell types outside of endothelial cells (ECs), such as smooth muscle cells (SMCs). Abnormal SMC proliferation is a characteristic

Extracellular sulfatase 2 (SULF2) is an extracellular protein highly expressed in many organs and tissue, such as the heart.

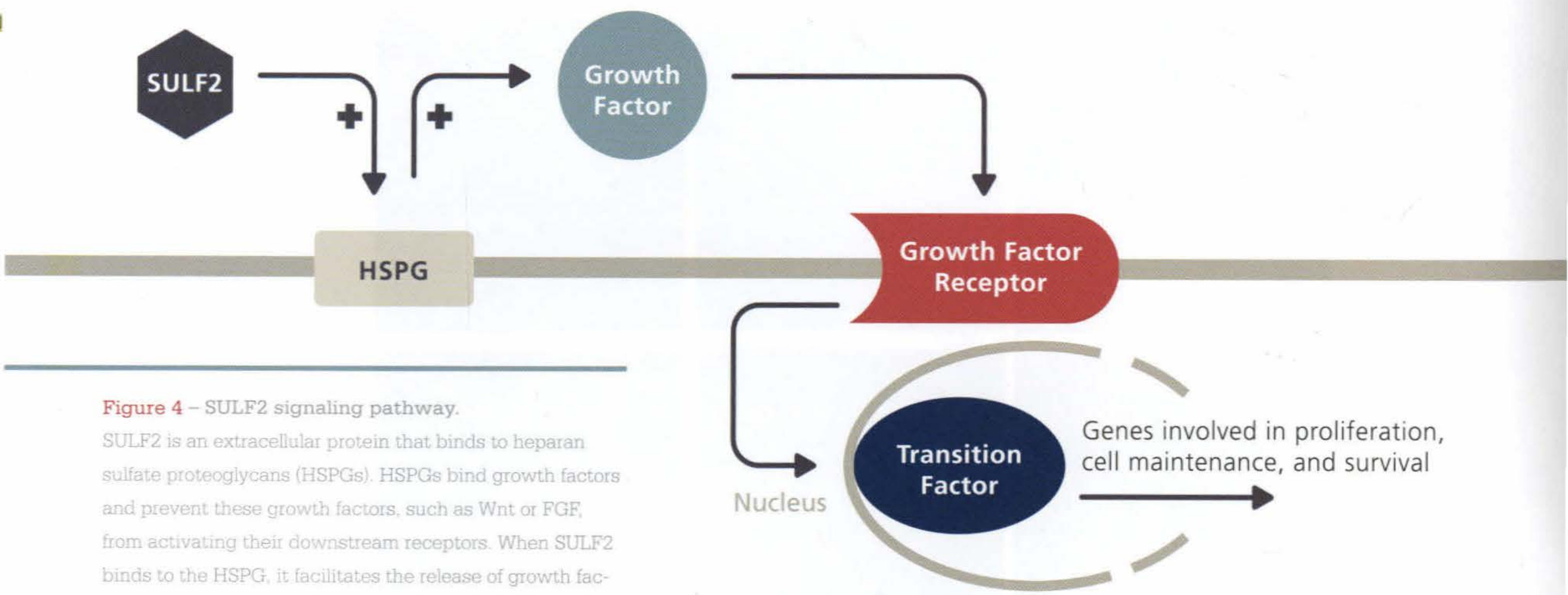

Figure 4 – SULF2 signaling pathway.
SULF2 is an extracellular protein that binds to heparan sulfate proteoglycans (HSPGs). HSPGs bind growth factors and prevent these growth factors, such as Wnt or FGF, from activating their downstream receptors. When SULF2 binds to the HSPG, it facilitates the release of growth factors, which activates cell-signaling pathways. This eventually leads to activation of a transcription factor in the nucleus, which leads to the transcription of genes involved in cell proliferation, maintenance, and survival.

feature of pulmonary hypertension that contributes to the harmful remodeling of the blood vessels. It is possible that upregulated SULF2 is released by the ECs and eventually binds to the HSPGs on the SMCs, thus leading to activation of growth factor signaling pathways and increased SMC proliferation. Therefore, it will be important to assess the levels of SULF2 protein in the medium in which the ECs are cultured to see if SULF2 is indeed being released by the ECs. It will also be important to see if the SULF2 protein from ECs actually affects the proliferation of SMCs by culturing control and patient SMCs in EC medium in which patient IPAH cells were grown.

It is interesting to note that while the full-length SULF2 protein is 98 kDa, the antibody used for the immunoblotting detects the protein at 49 kDa. The most likely explanation for this difference is that SULF2 is synthesized as a multi-domain protein, which is then cleaved by proteinases to form heterodimers consisting of 75 and 50 kDa subunits. The 50 kDa subunit, which appears to be the protein subunit detected in this western blot, is necessary for sulfatase activity. If this 50 kDa subunit is active and released from the ECs, it may contribute to the excess proliferation of SMCs as seen in IPAH.

Based on the results of the immunofluorescence, it appears that the fragment of SULF2 that has been detected is primarily nuclear. The non-permeabilised patient cell lines also show some cytosolic/extracellular staining that was not observed in the non-permeabilised control cell lines. However, previous research has only shown SULF2 to be an extracellular protein, so it is possible 50 kDa fragment that is localizing to the nucleus has a different function from the extracellular protein.

FURTHER READING:

Rabinovitch, M. 2008. Molecular pathogenesis of pulmonary arterial hypertension. J Clin Invest 118:2372-2379.

Humbert M et al. 2004. Cellular and molecular pathobiology of pulmonary arterial hypertension. J Am Coll Cardiol. 43(12 Suppl S):13S-24S.

Lai JP et al. 2010. The oncogenic effect of sulfatase 2 in human hepatocellular carcinoma is mediated in part by glypican 3-dependent Wnt activation. Hepatology. 52(5):1680-9.

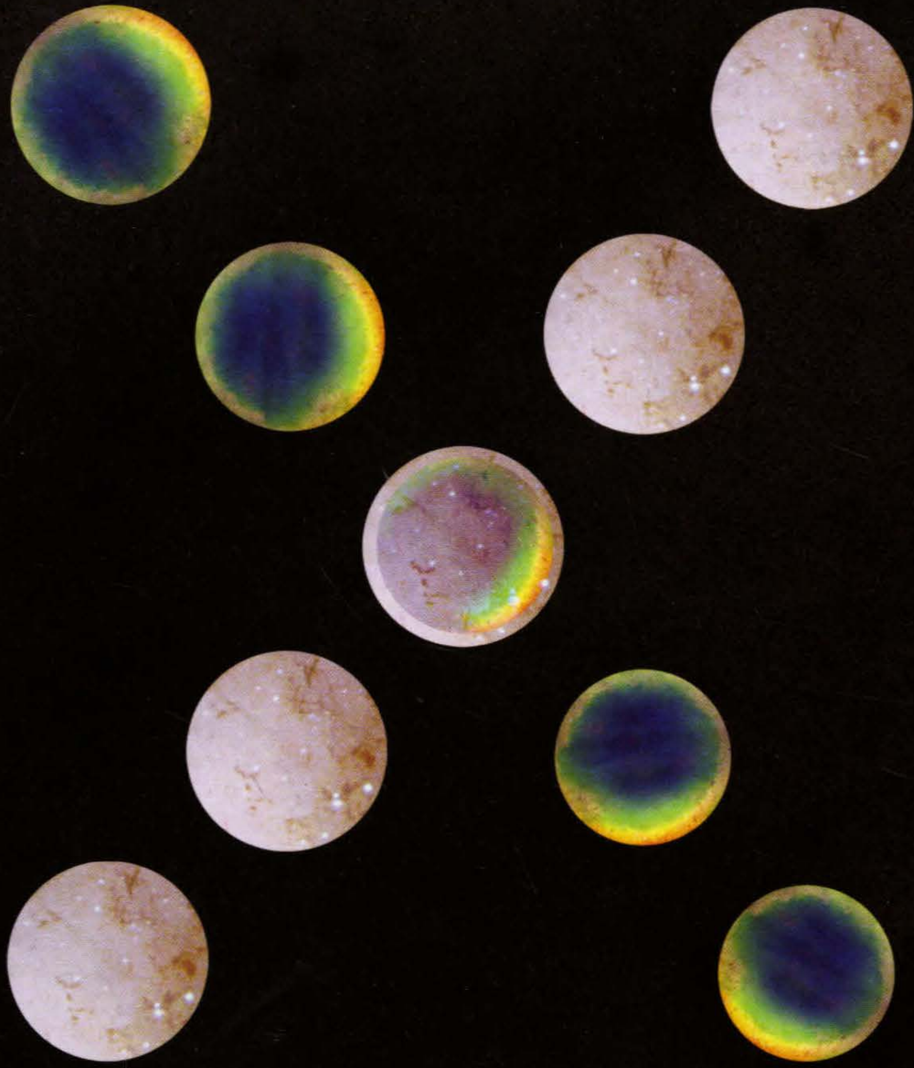

MARKS THE SPOT

This project aims to find binary systems of white dwarfs (WDs) in which the primary and the companion eclipse each other. In this project, we used Palomar Transient Factory (PTF) photometry cross-matched with SDSS white dwarfs and looked for candidates of eclipsing binary systems. We found three white dwarf M-Dwarf binary systems that are possibly eclipsing and three variable WD-WD binaries. We also found candidates for pulsating WDs with DQ, DZ, and DC spectral classification.

ECLIPSING BINARY WHITE DWARFS IN ARCHIVAL PALOMAR TRANSIENT FACTORY DATA

Suhail Dhawan
Mentor:Shrinivas Kulkarni
Co-mentor:Shriharsh Tendulkar

1 INTRODUCTION

White dwarfs (WDs) are compact objects that are formed when the fusion reactions cease in cores of stars with intermediate masses. We looked for detached binary systems in which both components are WDs that eclipse each other during an orbital revolution. Such systems are hard to find because the inclination of the orbit must be perpendicular or nearly perpendicular to the line of sight of the observer in order to see the eclipse. We have only three previous instances of such systems being found ([1], [2], [3]). The light curve of the system from [1] is shown in Figure 1 (on the following page).

Eclipsing binary white dwarfs are interesting astronomical laboratories. One can determine orbital parameters, as well as masses and radii of compo-

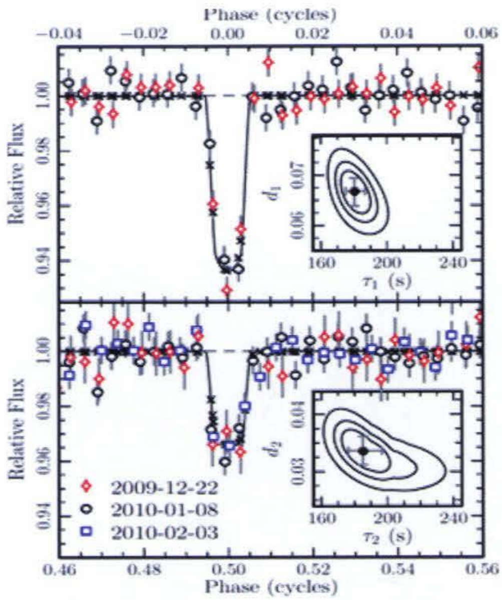

▲ *Figure 1: Steinfadt et al. (2010) Light Curve of NLTT 11748; the first ever eclipsing binary white dwarf system*

Figure 2: Source number 8377 from the SDSS WD catalog (top). The false positive from the absolute photometry (bottom) ▶

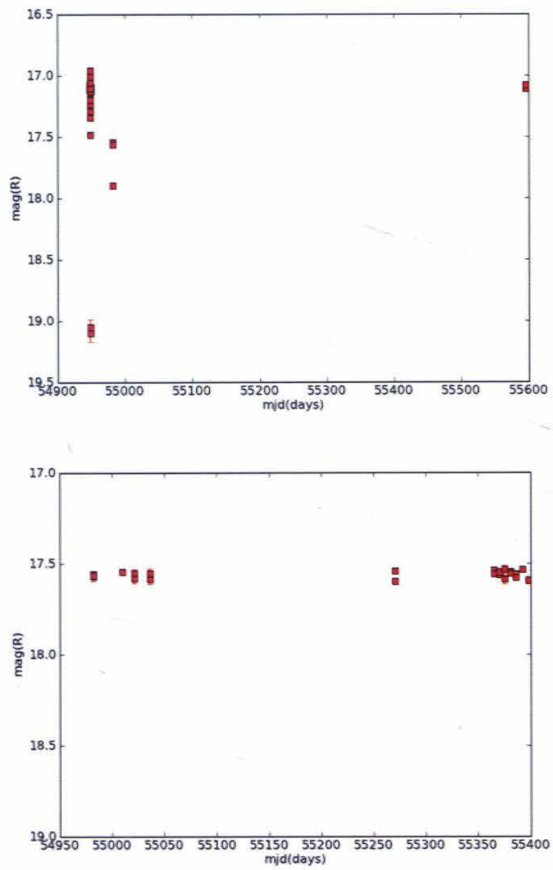

nent WDs, very accurately. Knowing these masses and radii, we can measure the age of our galaxy, identify cluster membership and determine distances to stars. A population distribution of binary white dwarfs can help us determine whether or not they are progenitors of Type 1a supernovae. Binaries with short enough periods (Brown et al. 2011) can provide evidence for gravitational radiation and are plausible candidates for a space based gravity wave detector. We looked for these systems in archival data of the Palomar Transient Factory.

1.1 PALOMAR TRANSIENT FACTORY

The Palomar Transient Factory is a 12KX8K CCD array re-engineered for the 1.2m Oschin-Schmidt Telescope at Palomar. It surveys large areas of the sky at varying cadences. Apart from a five-day cadence supernova search, the project looks for exotic transients.

PTF has a very large field of view of 7.2 square degrees. It observes 10,000 objects per exposure. A sum total of 250 million objects have been observed by the project, corresponding to a total of 3 billion data points.

2 PROJECT WORK

In this SURF project, we aimed to use archival data from the Palomar Transient Factory and cross-match it with the catalog of SDSS confirmed white dwarfs (S. J. Klienman, private communication). Those WDs observed by PTF were analyzed for variability. Candidates with interesting light curves were listed for follow-up observation like radial velocity measurements and detailed photometry.

After cross-referencing the SDSS confirmed WDs, we selected those targets with sufficient amount of data. With these candidates, we truncated the number based on variability cut, selecting sources where the difference between the minimum and maximum brightness was greater than 5 times the standard deviation. For those WDs that met this criterion, we looked at the light curves manually. Upon matching/recalibration for a few of the interesting sources we saw that some candidates

"BINARIES WITH SHORT ENOUGH PERIODS CAN PROVIDE EVIDENCE FOR GRAVITATIONAL RADIATION."

showing variability were actually stable stars (see Figure 2). The absolute photometry was yielding false positives.

2.1 RELATIVE PHOTOMETRY

To solve the problem of false positives, we wrote a code for a relative measure of magnitude for the WDs. This code corrects for the errors using a comparative measurement with respect to the stars in the neighbourhood of the target object. To obtain the correction for each observed magnitude of the source, we first obtain all the data for a large number of stars in the neighbourhood of the object.

We calculate the median magnitude for each star and the difference of each observation from this median magnitude, calling it a certain delta magnitude.

$$Mag_{exposure,n} - Mag_{median,n} = \delta Mag_n \quad (1)$$

For all the stars (say, a total of n in number)in consideration we take a median value of the delta magnitudes for a given exposure or observation and call it the zero point correction for that exposure.

$$Median(\delta Mag_n) = ZeroPointCorrection \quad (2)$$

We then add this correction to the magnitude of the source for that particular exposure. The light curve then plotted is of these corrected magnitudes with respect to the epoch of observation.

$$Mag_{absolute} + ZeroPointCorrection = Mag_{relative} \quad (3)$$

2.2 FURTHER ANALYSES

Those candidates that showed variability in the light curves after zero point corrections were then analysed further to confirm the variability. We ran a chi square test with a null hypothesis that the star is stable. For values of the chi square statistic greater than 5 we considered the candidate as a deviation from the null. Candidates above the chi square threshold value were then analyzed for periodicity using the Lomb-Scargle periodogram. Sources showing a sharp peak at one value were then folded about that peak and then plotted as a phase binned light curve. For these analyses, we converted to a heliocentric reference frame in order to correct for the earth's revolution about the sun. This is important since the data we have obtained is over a period of hundreds of days.

3 RESULTS

After analyzing the light curves, we found the following interesting candidates. 3 WD-WD binaries that were spectroscopically confirmed by the ELM survey showed variability in PTF. One of them appears to be the first ever system of a pulsating hydrogen spectrum (DAV) WD in a binary. Multiple white dwarf M-dwarf (WD-MD) binaries show variability. The most interesting of those is shown in Figure 3.

About 15 carbon spectrum (DQ) WDs show variability. We also found 5 metallic spectrum (DZ), 4 continuum spectrum (DC), 3 helium spectrum (DB) and 2 carbon/oxygen spectrum (DO) WDs showing variability. We also found DA (hydrogen spectrum) WDs showing interesting dips. WDs with more than one letter describing their spectral type (ex. DBAZ, DBAH) were also seen to be having outliers.

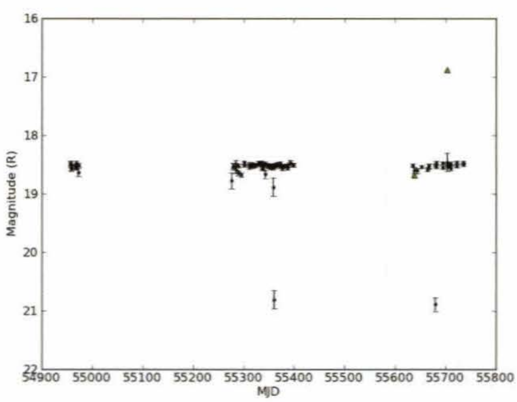

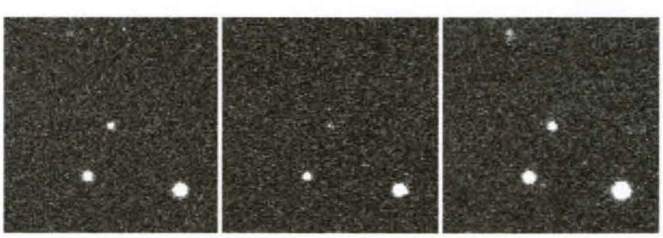

Figure 3: The light curve shows two points that drop by 2 magnitudes (R-band). The cut-out images show the star, before, during and after the eclipse.

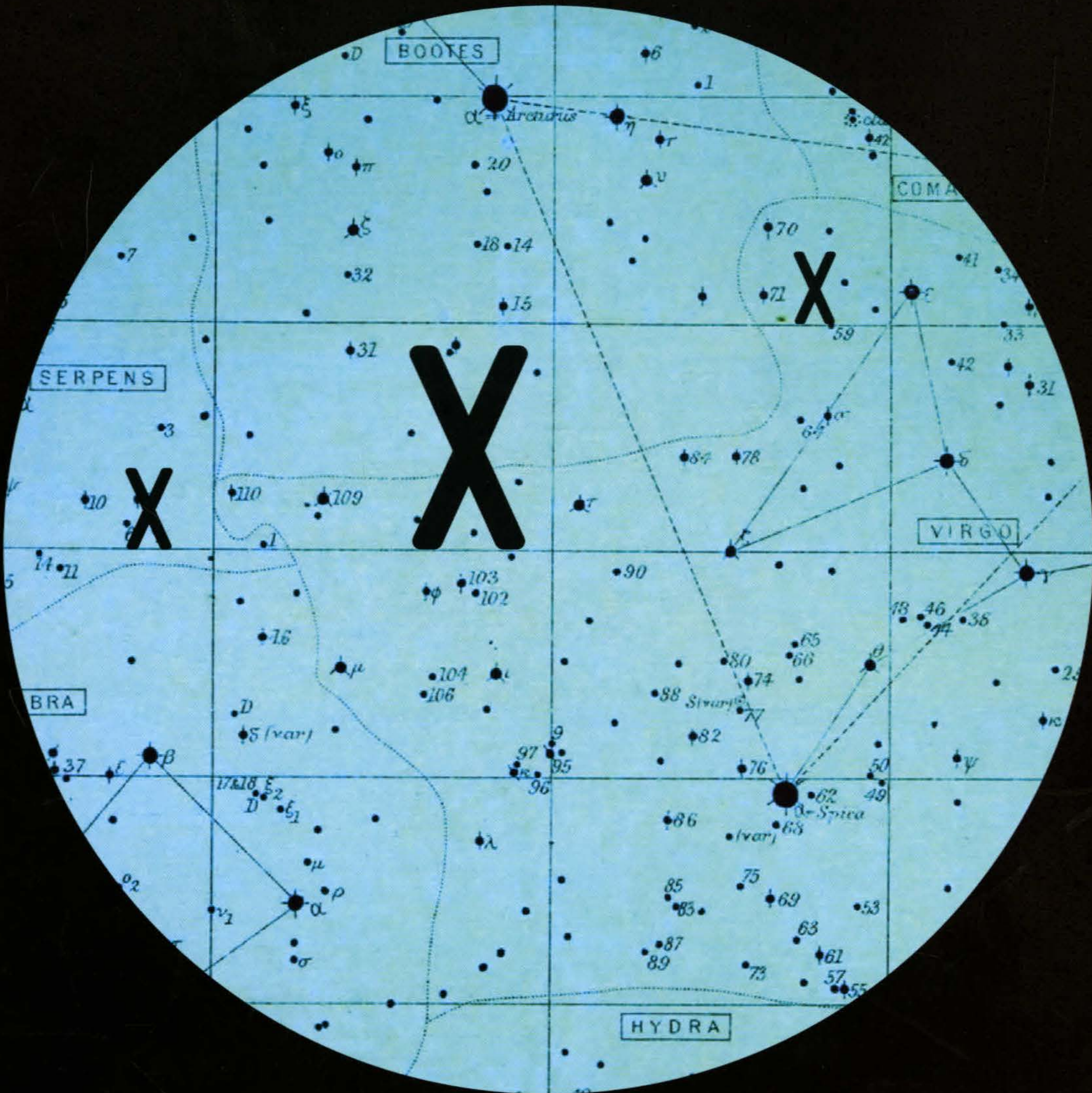
BOOTES
Arcturus
COMA
SERPENS
VIRGO
Spica
HYDRA

4 CONCLUSION AND DISCUSSION

After the 10 weeks of work, we have a candidate list of near 100 WDs that are showing interesting variable features. They have been stored in the PTF galactic marshal and the most intriguing ones will be followed up.

Systems like the DAV in a binary could offer great insight into the evolution of a WD-WD binary. A measurement of the modes of pulsation of the binary can help us determine the mass of the outer hydrogen layer of the white dwarf.

DQ variable WDs are interesting because currently there are only 4 such objects known and there exists no theoretical explanation for why they should be variable and there are no correlations between the periods and amplitudes of the known ones [4]. DZ variables are of interest because no such system has been found previously and no existing reasoning for why they should vary.

5 ACKNOWLEDGEMENTS

I would like to thank my mentor:Prof. Shrinivas Kulkarni, my co-mentor: Shri- harsh Tendulkar, Prof. Paul Groot, David Levitan, Varun Bhalerao, Eran Ofek and Branimir Sesar for their help during my research. I would also like to thank the SFP office.

6 FURTHER READING

1. Steinfadt, J. D. R., et al., ApJ Lett, 716, 2, L146-L151 (2010)
2. Parsons, S.G.,et al.: arXiv:1105.3946
3. Brown et al.: arXiv:1107.2389
4. Dunlap, B.H., et al. ApJ Lett, 720, 2, L159-L163 (2010)

Interview with Jacqueline Barton

As an undergrad, what areas were you interested in, and how did that evolve over time? Did you have an idea you would go to grad school?

I didn't take chemistry in high school. I took more math, and then, when I went to college, I started to take chemistry and loved it. It's math, except you can go into the lab and do reactions. When I finished college, I thought I might be a college professor in a small school, and so every summer I did research. In graduate school I first thought I'd like to do statistical mechanics because I was still interested in math. Then, Steve Lippard, a bioinorganic chemistry professor at Columbia U, had a project on metal complexes binding to DNA. He sort of pitched it to me as a one-dimensional cooperative distribution problem, so it had a statistical component to it. That's how I started to get into DNA.

What does it feel like to be awarded the National Medal of Science?

It feels nice. It is as much an honor for my students in my lab. The ceremony was broadcast live, and they were watching it in the lab. I don't know if you know, but my husband, Peter Dervan won it too. As a family, it was great to do it again.

What was it like to meet President Obama?

It was great. He was tall. He's cordial, as one would expect. I had a short one-on-one time with him, but one thing I did ask was if his daughters are interested in science. A smile lit across his face

You and your lab must have completed a countless number of experiments. Could you tell us about your research in very lay terms and the path you took to achieve this award?

Henry Taube had carried out many experiments looking at electron transfer reactions between metal complexes in solution, and Rudy Marcus developed his electron transport theories based on those experiments. I had a postdoc in the group, Vijay Kumar, who asked what would happen if we did similar electron transfer reactions between similar metal complexes but in the presence of DNA, and it seemed like a nice easy experiment to do. Other scientists had asked, essentially since the 1950s, if DNA could facilitate electron transfer? We did the experiment, and what we found was that the reaction was more efficient in the presence of DNA than in the absence of DNA. I was sure that that was the case because since the metal complexes were positively charged, they would move along the DNA polyanion easily, essentially reducing a three-dimensional search to a one-dimensional search.

In fact, what we found was that that the reaction was even better and that maybe they weren't using DNA as a railroad track in a facilitated search, but maybe instead as a wire. Electrons could migrate from one complex to another through the base pair stack. We then did an experiment in which we tethered one metal complex to one end of DNA and another complex to the other end of DNA, and we showed that we had photo-induced quenching of one metal complex by the other via electron

transport. We then also used biochemical methods to analyze damage to DNA from photooxidation from a distance, and the damage that we found was also consistent with long range migration of electrons.

Other scientists were skeptical and thought that maybe the DNA is bending in some way, bringing the oxidant and reductant together on the DNA? But these are short oligonucleotides, and they weren't going to bend. I was a nucleic acid chemist, and I understood that. So then, we put a bend in the DNA intentionally; we put an extra few bases on one strand in the DNA to interrupt the stacking, and when you kinked the DNAin that way, we didn't get the long range effects. So, that supported the hypothesis that it was going through the DNA.

We did another even subtler experiment, and we put in a base-base mismatch, instead of a bend. The mismatch was a subtle change in stacking, but enough to turn off the electron transfer. We said, gee, this is an interesting reaction that we can use to detect things like mismatches. We have now shown that electrons can go through 100 base pairs or 34 nanometers of well stacked DNA, as long as there's not a mismatch. If there's a mismatch, it turns it off just as it does in a smaller piece of DNA. DNA is actually currently the longest documented molecular wire.

We started saying this could be really good for making sensors for DNA binding proteins and for detecting mutations for DNA. Then, we started wondering if nature uses this reaction. It turns out that there's a subset of proteins that repair mistakes in DNA and these repair proteins have iron-sulfur clusters in them; iron-sulfur clusters in other proteins commonly carry out electron transfer chemistry. We're finding that these repair proteins bound to DNA have just the right potential and just the right redox characteristics to carry out electron transfer chemistry on DNA.

Our current model for how these repair proteins find mistakes in DNA is like two telephone repair-men finding a mistake in the line. How do they find a break in the wire? One fellow gets up on a ladder and the other repairman gets up on a ladder someplace else, and if they can talk to each other through the line, everything's fine on the line. If they can't talk to each other, then they can hone in on where the mistake is. We actually think repair proteins do the same thing. If they can talk to each other, using electron transfer chemistry, then the DNA is intact. If they can't talk to each other, then there must be some lesion in the way that's hindering electron transfer. Now, we're seeing in the literature that there's a whole variety of DNA-binding proteins being discovered that have iron-sulfur clusters, and we think that this may be chemistry being used by nature for signaling across the genome. When the cell is under stress and you want to coordinate the response, you want to do it across the genome - activate repair, activate transcription or what have you. That's what we're up to now.

Young scientists like us aspire to succeed like you have. What advice do you have for us?

My advice is to follow your gut. Life ends up being a series of accidents, and you sort of go from one thing to another. I did not have a plan when I was your age and I didn't know that I was going to end up here in this office and in this circumstance, but if you do what you love, you end up doing it well. It's harder to do something well when you don't like doing it. So, just listen to what you love, and it all works out.

CURJ's goal is to publish significant undergraduate research. What are some of your views on undergraduate research experiences, and how does it shape future scientists?

I think there's nothing more important than getting in the lab and doing research. Undergraduate research in the summer and during the year is what got me excited about science. It wasn't reading books and doing that stuff. It's getting in the lab and watching a reaction, and that's what really shapes you. I would bet that all my colleagues in the CCE division had the same experience; it starts as an undergraduate doing research. That's when you find something that you love, and you just want to keep on doing it. The wonderful thing about research is that you don't know the answer, and so you ask another question. You've got to be asking questions you don't know the answer to because if you know the answer already, you're asking the wrong question. And, following up and discovering all these things you didn't know is incredibly exciting. It can get frustrating because there's a lot of times the experiment doesn't work, and you've got to do another experiment and redesign it. Like the experiments that we first did, some scientists didn't buy into it, but that just made us design better and better experiments. So, it can be frustrating, but when you get the result, that's really cool.

"Follow your gut. Life ends up being a series of accidents... but if you do what you love, you end up doing it well."

Reach New Heights

Our Employees:

- Utilize advanced techonologies
- Thrive in a fast-paced environment
- Are rewarded for innovation & success

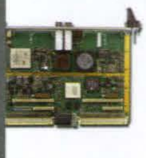

Curtiss-Wright Controls is:

- Electronic System Solutions
- Ground, sea and air platforms
- Global leader with 100+ years of history

CURTISS WRIGHT Controls
Electronic Systems

Curtiss-Wright is an Equal Opportunity Employer

cwcelectronicsystems.com/careers.html

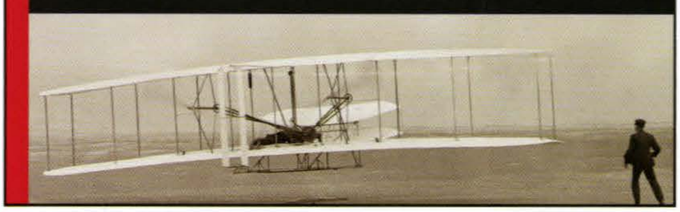

GENERAL DYNAMICS
Electric Boat

Get your career underway

The Nuclear Submarine Has Long been the silent backbone of United States Naval Supremacy. ***ELECTRIC BOAT*** designs and builds these incredible machines.

We are looking for energetic and innovative individuals to continue the tradition of excellence that has become synonymous with ***ELECTRIC BOAT***. We will show you how to apply your skills to the art of nuclear submarine design, engineering and construction.

ELECTRIC BOAT has immediate openings in Groton, Connecticut, for entry level engineers with zero to three years experience.

ELECTRIC BOAT is looking for engineering candidates with a minimum of a Bachelors degree in:

• Aerospace • Chemical • Civil • Computer • Computer Science • Electrical • Mechanical • Marine/Ocean • Naval Architecture

ELECTRIC BOAT offers an excellent salary and benefits package, including Tuition Reimbursement, Relocation assistance, and an excellent 401K Plan.

GENERAL DYNAMICS
Electric Boat
75 Eastern Point Road
Groton, CT 06340-4989

Please visit www.gdeb.com/employment for more information, or contact Electric Boat Employment office at 1-888-231-9662

US Citizenship Required Equal Opportunity / Affirmative Action Employer

---

INSTITUTE FOR
Systems Biology
Revolutionizing science. Enhancing life.

The Institute for Systems Biology (ISB) is an internationally renowned non-profit research institute dedicated to the study and application of systems biology. Our goal is to unravel the mysteries of cellular networks and identify strategies that will usher in a new era of P4 Medicine (predictive, preventive, participatory, and personalized medicine).

ISB is committed to transforming science and medicine in the 21st century by engaging leading-edge investigators from diverse disciplines and backgrounds. Our small and highly-focused teams work in a collaborative environment that fosters innovation and creativity. ISB's multi-disciplinary approach enables investigators to develop and integrate unique perspectives, tools and strategies required for tackling complex biological problems and create novel technologies that will invent the future.

ISB's approach to research, coupled with a culturally diverse employee population, creates a stimulating and inclusive environment. ISB values diversity and is committed to equality of opportunity and promoting the development of its employees to achieve their fullest potential.

Visit our website for additional information and career opportunities.

www.systemsbiology.org

★ Institute for Defense Analyses ★

For over half a century, the Institute for Defense Analyses has been successfully pursuing its mission to bring analytic objectivity and understanding to complex issues of national security. IDA is a not-for-profit corporation that provides scientific, technical and analytical studies to the Office of the Secretary of Defense, the Joint Chiefs of Staff, the Unified Commands and Defense Agencies as well as to the President's Office of Science and Technology Policy.

To the right individual, IDA offers the opportunity to have a major impact on key national programs while working on fascinating technical issues.

broaden your perspective | **IDA**

your career • your future • your nation

IDA is seeking highly qualified individuals with PhD or MS degrees

Sciences & Math	Engineering	Other
• Astronomy	• Aeronautical	• Bioinformatics
• Atmospheric	• Astronautical	• Computational Science
• Biology	• Biomedical	• Computer Science
• Chemistry	• Chemical	• Economics
• Environmental	• Electrical	• Information Technology
• Physics	• Materials	• Operations Research
• Pure & Applied Mathematics	• Mechanical	• Statistics
	• Systems	• Technology Policy

Along with competitive salaries, IDA provides excellent benefits including comprehensive health insurance, paid holidays, 3 week vacations and more – all in a professional and technically vibrant environment.

Applicants will be subject to a security investigation and must meet eligibility requirements for access to classified information. U.S. citizenship is required. IDA is proud to be an equal opportunity employer.

Please visit our website www.ida.org for more information on our opportunities.

IDA Please submit applications to: http://www.ida.org/careers.php

Institute for Defense Analyses 4850 Mark Center Drive Alexandria, VA 22311

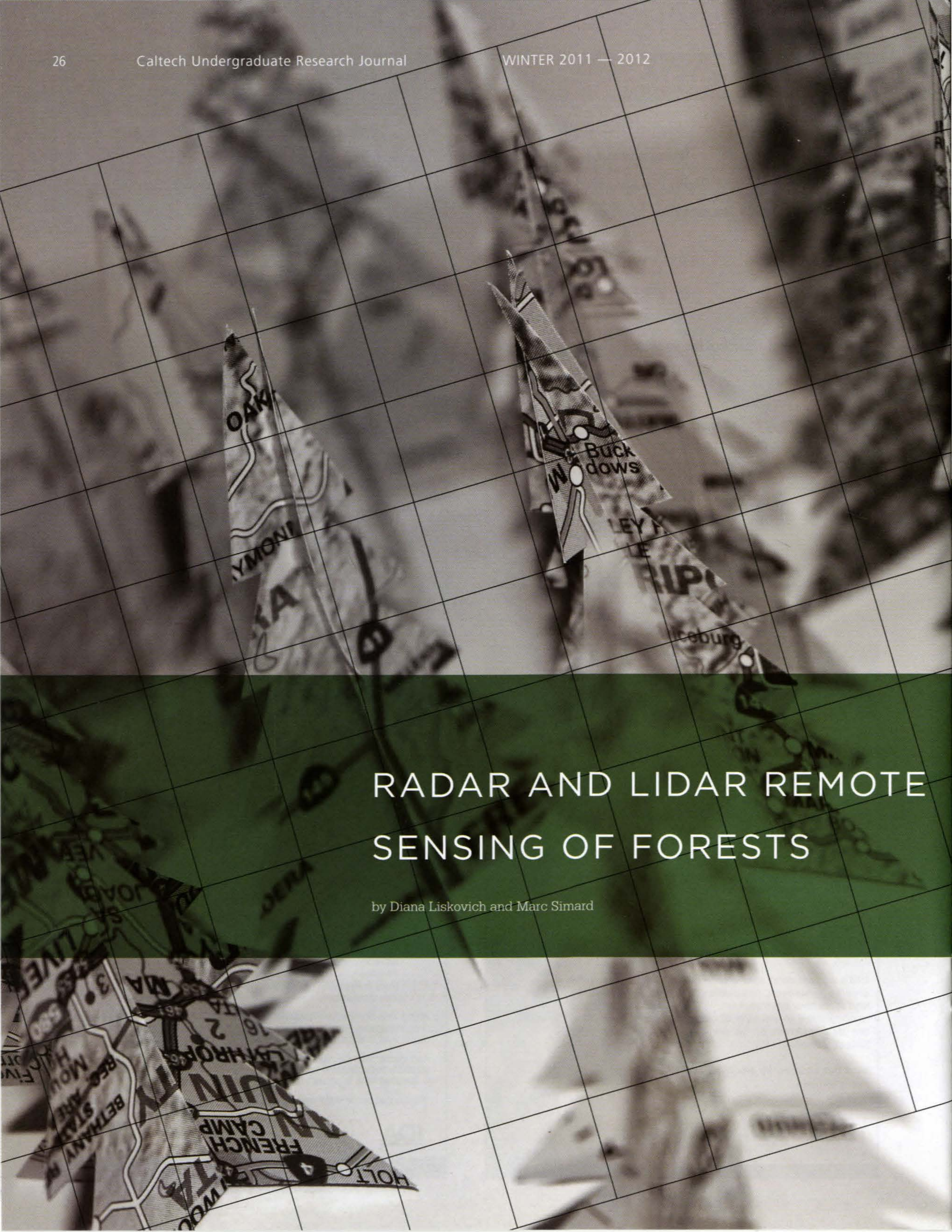

RADAR AND LIDAR REMOTE SENSING OF FORESTS

by Diana Liskovich and Marc Simard

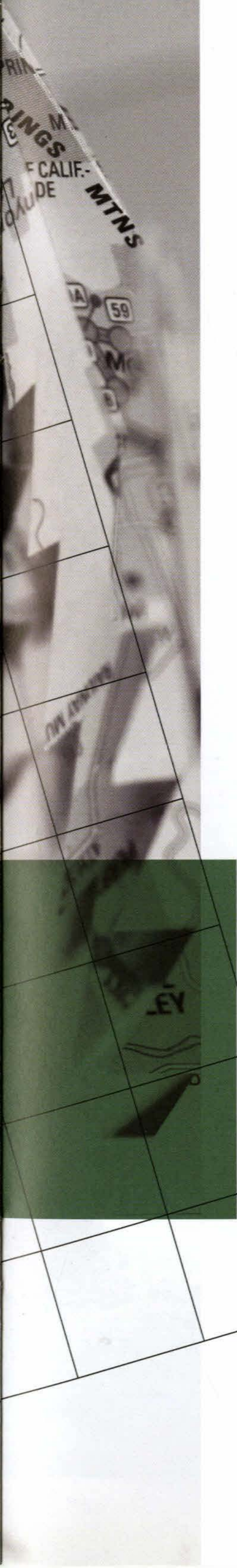

INTRODUCTION

Digital elevation models are three dimensional representations of terrain, depicting the topography of the region with exacting detail. However, the accuracy of the models declines in forest-type territories, due to the difficulty of mapping forestial structures. Using radar and lidar data, the aim is to improve 3D rendering of terrain, including digital elevation models (DEM) and estimates of vegetation height and biomass in a variety of forest types and terrains. The 3D mapping of vegetation structure and the analysis are useful to determine the role of forest in global warming (carbon cycle), in providing habitat and as a provider of socio-economic services. This in turn will lead to potential for development of more effective land-use management.

A CONVENIENT SOLUTION

The first objective was to perform an analysis of how digital elevation model (DEM) error varies geographically and with vegetation cover. Using python programming language, the variation of DEM error with latitude, canopy height, signal to noise ratio (SNR), number of lidar waveform peaks, and maximum peak width were analyzed. The data were then fitted with 1st degree and 2nd degree polynomials. To inspect higher order trends, the data was plotted with a mean, median, and variance filter. The density of data points was analyzed as well. The data was filtered to get rid of very high values that may indicate an incorrect measurement or measurement of a cloud rather than a canopy. Both the filtered and unfiltered data were considered and analyzed. Finally, the variation of DEM error with latitude and longitude was examined and represented by a color coded map.

THE APPROACH

In order to perform DEM error analysis, we used three different data sets: L2C, L3C, and L3F, which are obtained from specific ICESat/GLAS lasers. The data was filtered to get rid of very high values that may indicate an incorrect measurement or measurement of a cloud rather than a canopy. Plots were then created for both the filtered and unfiltered data. For both filtered and unfiltered data, points with absolute DEM error values greater than 32000 meters were eliminated. For only the filtered data, points with absolute DEM error greater than 100 meters were eliminated. For each data set, we split the globe up into three regions and plotted the relationship for each individual region. The three regions are 1: North America and South America (between the longitudes of -180 and -28), 2: Europe and Africa (between the longitudes of -28 and 53), 3: Asia and Australia (between the longitudes of 53 and 180). We had data for latitudes greater than 60 degrees and less than -60 degrees,however, additional density plots were created only for points between the latitude

NOMENCLATURE

DEM	= digital elevation model
SRTM	= Shuttle Radar Topography Mission
ICESat	= Ice, Cloud and land Elevation Satellite
GLAS	= Geoscience Laser Altimeter System
SNR	= signal to noise ratio
LiDAR	= light detection and ranging
RH100	= (100% waveform energy)
RH75	= (75% waveform energy)
LVIS	= Laser Vegetation Imaging Sensor
L2C	= Specific ICESat/GLAS laser
L3C	= Specific ICESat/GLAS laser
L3F	= Specific ICESat/GLAS laser
inSAR	= Interferometric Synthetic Aperture Radar
UAVSAR	= Uninhabited Aerial Vehicle Synthetic Aperture Radar

values of -60 and 60 since Shuttle Radar Topography Mission (SRTM) does not gather data past these latitude values. All of these plots were created by writing computer programs in the Python programming language.

A. DEM Error

DEM error was calculated using Ice, Cloud and land Elevation Satellite (ICEsat) and SRTM elevation estimates. The equation used was:

(DEM error) = (SRTM elevation) – (ICEsat elevation)

SRTM was launched February 11th, 2000. It flies around the Earth thus creating maps on global scales. SRTM uses interferometry to gather elevation height data. The shuttle has two antennas, both of which receive radar signals. However, only the main antenna transmits and receives signals. The technique used to measure elevation is called fixed-baseline interferometry. Here two radar data sets are collected simultaneously – one by the outboard antenna and one by the onboard antenna. The onboard antenna sends a radar beam and scattered rays are collected by both antennas. The distance between the two antennas is kept constant, what changes is the distance to the Earth from each antenna. Using the phase difference between the 2 data sets and the baseline length, the elevation can be calculated.

Launched on January 13th, 2003, the ICESat carries the Geoscience Laser Altimeter System (GLAS). The laser altimeter emits laser pulses of 5 nanosecond duration to the Earth's surface and then measures the amount of time it takes for that pulse to return to the satellite. With known time and speed of light, the round trip distance can be calculated. Using a Global Positioning System (GPS) receiver and star cameras and gyroscopes carried on the instrument, the laser direction in space is determined. Knowing the satellite position and the laser pointing direction allows calculation of the exact position on Earth which laser pulse illuminates. Finally, the combination of many of these footprints provides an image of the topography of the Earth.

B. Tales of Two Variables

For the purposes of this experiment, the dependent variable is DEM error. The independent variables are latitude, maximum peak standard deviation, number of peaks, RH100, RH75, and SNR. The three different data sets used represent three different lasers that are used onboard ICEsat/GLAS to obtain measurements and waveforms. ICESat/GLAS carries three lasers, each which have two lidar channels, one 1064nm for surface altimetry and dense cloud heights, and another 532nm for vertical cloud and aerosol distribution. To increase the lifespan of the mission, each laser is operated one at a time several times a year for 33-56 day periods. L2C is data obtained from the second laser when it was operated for 35 days between the dates of May 20 2005 and June 23rd 2005. L3C is data obtained from the third laser when it was operated for 35 days between the dates of May 18th 2004 and June 21st 2004. L3F is data obtained from the third laser when it was operated for 33 days between the dates of May 24th 2006 and June 26th 2006.
Each independent variable was plotted against the DEM error. For each, scatter plots with 1st and 2nd degree polynomial estimation were created, as well as density plots, mean, median, and variance plots.

Finally, the combination of many of these footprints provides an image of the topography of the Earth.

C. Latitude

Latitude ranges from -90 to 90 degrees. However, SRTM only measures elevation between the latitude ranges of -60 and 60 degrees. This is reflected in the analysis because latitudes outside of that range were ignored. For all three different data sets: L2C, L3C, and L3F, the relationship between DEM error and latitude appeared similar.

From the graph of data points in North America and South America (Figure 1), it can be seen that a majority of points have a DEM error of zero meters. Some data that is not depicted in the plot because of the existence of unreasonably high values, which can be attributed to a cloud reading rather than a forest canopy reading. The other two regions – Africa and Europe, and Asia and Australia – exhibited similar behavior. The data points were concentrated around where DEM error equals zero.

To see if there were higher order relationships, the mean of DEM error was plotted against Latitude. The plotted relationships for North America and South America, Europe and Africa, and Asia and Australia are in Figure 2. The graphs show that there is a negative spatial correlation between DEM error and latitude. There are also patches of either positive or negative DEM error values. A potential explanation could be the fact that where forests exist, the radar penetrates further down in the forest whereas the lidar reads mostly only the canopy heights. Therefore wherever there are forests there would either be consistent positive or negative DEM error values.

D. Maximum Peak Standard Deviation

The maximum peak is the largest peak of the received waveform, and the standard deviation of that peak signifies its width. The relationship between max peak standard deviation and DEM error remained the same for all three L2C, L3C, and L3F data sets. It also was generally the same for all the three regions: North and South America, Africa and Europe, and Asia and Australia. As evident from the density plot on the upper right, the concentration of data points was around a DEM error of zero and a Maximum Peak Standard Deviation of zero. However, as DEM error increased and maximum peak standard deviation increased, the density of points decreased. This is evident in the unfiltered data as well. The red line in the scatter plots, representing second degree polynomial estimations, shows that as maximum peak standard deviation increases (Figure 3), DEM error becomes more negative, or in other words, absolute DEM error increases. The mean, median, and variance data confirm this relationship (Figure 4), showing that as maximum peak standard deviation increase, so does absolute DEM error.

E. Number of Peaks: Canopy Features

The number of peaks represents the number of peaks in the waveform and ranges from integers between 1 and 6. Effectively, it shows if there are layers below the top canopy. The first peak is the top of the canopy and the last is the ground floor, and the peaks in between represent the forest understory. The relationship between the number of peaks and DEM error also did not vary much with data set or region, thus only the North America and South America plot is shown (Figure 5). From the density and scatter plots (not shown), the point distribution is centered at a DEM error of zero. The first and second degree polynomial estimates indicate no trends as well. The mean, median, and variance data do show as the number of peaks increases, the variation in DEM error increases. It also seems that there is usually a minimum value around where the number of peaks is equal to 5.

F. RH100: Canopy Height

RH100 signifies a value found by calculating 100% of the waveform energy, which is 100% of the area underneath the waveform. The density of points for both filtered and unfiltered data was found to be at DEM error = 0 meters and RH100 = 0 meters. The second degree polynomial fit shows that as RH100 increases, so does DEM error. The mean graph (Figure 6) shows

Figure 1

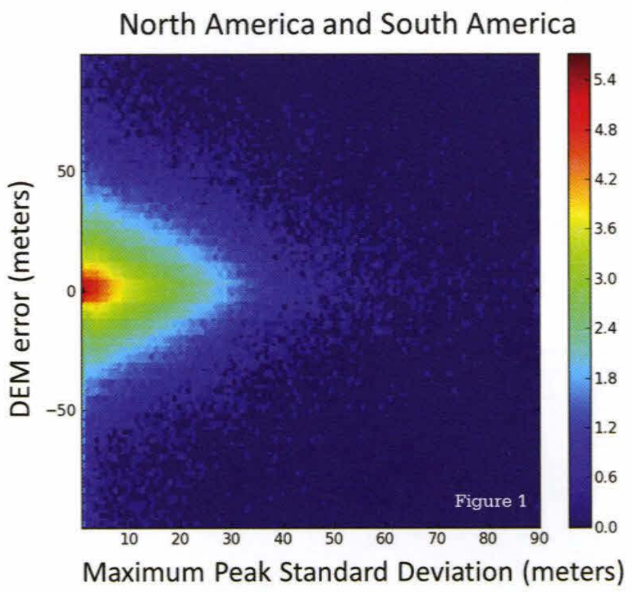

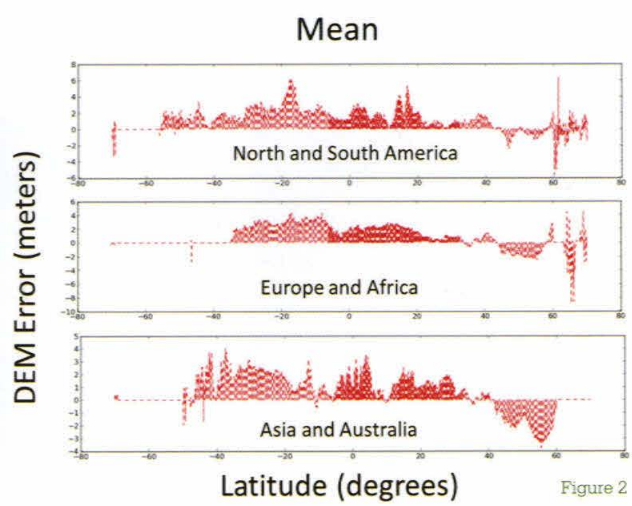

Figure 2

Fig 1: Color coded plot of DEM error versus latitude, depicting density of points of DEM error.

Fig 2: Three plots of the latitude verses the mean DEM error in North and South America, Europe and Africa, and Asian and Australia.

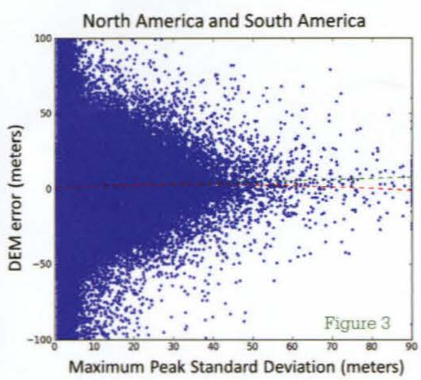

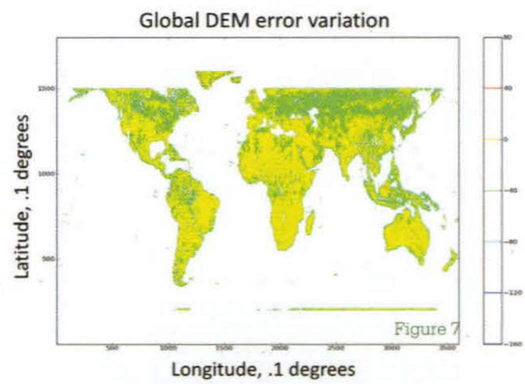

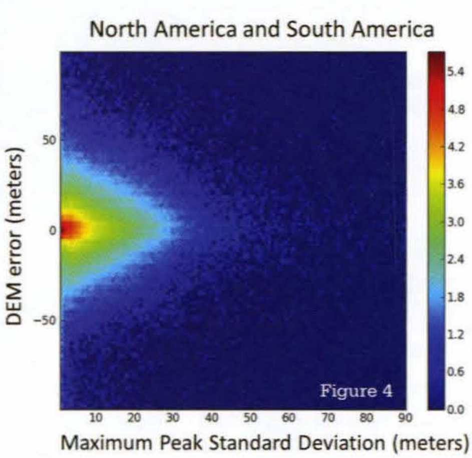

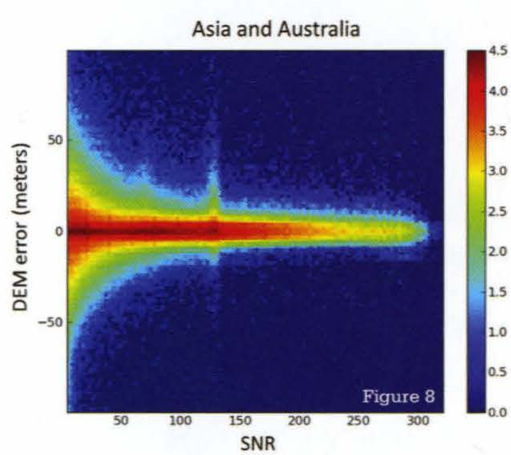

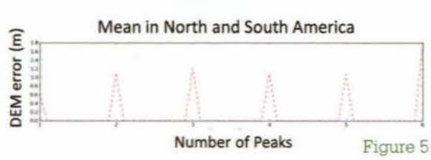

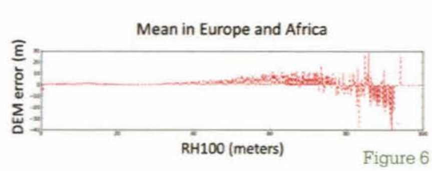

Fig 3: The red line in the scatter plots, representing second degree polynomial estimations, shows that as maximum peak standard deviation increases, DEM error becomes more negative, or in other words, absolute DEM error increases.

Fig 4: The density plot shows that DEM error is centered at DEM error = 0 and maximum peak standard deviation = 0.

Fig 5: Mean, median, and variance graphs for Number of Peaks versus DEM error for North and South America.

Fig 6: A plot of RH100 versus DEM error.

Fig 7: Density plot of filtered SNR data that shows points are concentrated around DEM error = 0.

Fig 8: Global map with colors signifying the magnitude of DEM error.

> There are a significant amount of values in the negative DEM error range scattered throughout the continents.

that as RH100 increases, absolute DEM error increases as well. However, the DEM error starts becoming more negative at around RH100 = 85-90 meters. The trend also stops before RH100 = 100 meters but that is probably due to the low quantity of data points with that value. For lower values of RH100 however, it seems there is no correlation between RH100 and DEM error. This holds true for all regions and data sets. The RH75 was calculated as well, with similar results and similar conclusions as compared to the RH100.

G. Signal-to-Noise Ratio

The SNR, or signal-to-noise ratio, compares the level of a desired signal to the level of background noise, meaning that if the ratio is lower, it signifies that there is more noise than signal, and vice versa. From the density plot (Figure 7), it is evident that a high density of points are concentrated around DEM error = 0. The mean, median, and variance data show that for each data set and region, DEM error is constant with varying SNR, however there is an increasing variance of DEM error with decreasing SNR values.

H. Global DEM Error

Figure 8 is a global map with colors signifying the magnitude of DEM error. It shows trends in global DEM error variation. On the map, blue and darker colors (values less than -100) signify no data. Yellow signifies zero DEM error. Green signifies negative DEM error values, and red signifies positive DEM error values. The map shows that a majority of the globe has a DEM error value of 0 meters. However there are a significant amount of values in the negative DEM error range scattered throughout the continents but concentrated in the north.

IF A TREE FALLS

Through investigating factors that may affect DEM error, we found that all the same trends were seen for all three data sets L2C, L3C, and L3F. The density of points for all the independent variables was concentrated where DEM error was equal to 0. Our analysis shows that there is a spatial correlation between DEM error and latitude, indicating a decreasing trend. For high values of RH100 and RH75, our analysis indicates that as RH increases, so does DEM error. This signifies that with greater canopy height, there tends to be greater DEM error. From the maximum peak standard deviation data, number of peaks, and RH data, the more forest or understory can be detected, the greater the DEM error is expected to be. The global map showed that a majority of the globe has a DEM error value of 0 meters. However, there are a significant amount of values in the negative DEM error range scattered throughout the continents, although it is mostly concentrated

Our analysis shows that there is a spatial correlation between DEM error and latitude.

in the northern hemisphere. Our findings show that there although a majority of our data have a DEM error of zero, there is a significant correlation between DEM error and each of our independent variables. In order to minimize DEM error, future investigations should be conducted in order to form theories that explain the existence of the correlations discovered in this experiment.

ACKNOWLEDGEMENTS

Diana Liskovich thanks Dr. Marc Simard for providing her with the opportunity to help with his work and for providing her with help and guidance along the way. She also thanks NASA's Universities Space Research Program for funding and making this research experience possible.

FURTHER READING

"DESDyni: Deformation, Ecosystem Structure and Dynamics of Ice," HYPERLINK "http://desdyni.jpl.nasa.gov/"http://desdyni.jpl.nasa.gov/

Duncanson L.I., Niemann K.O., Wulder M.A., "Estimating forest canopy height and terrain relief from GLAS waveform metrics," Remote Sensing of Envitonment, Vol 114, 2010.

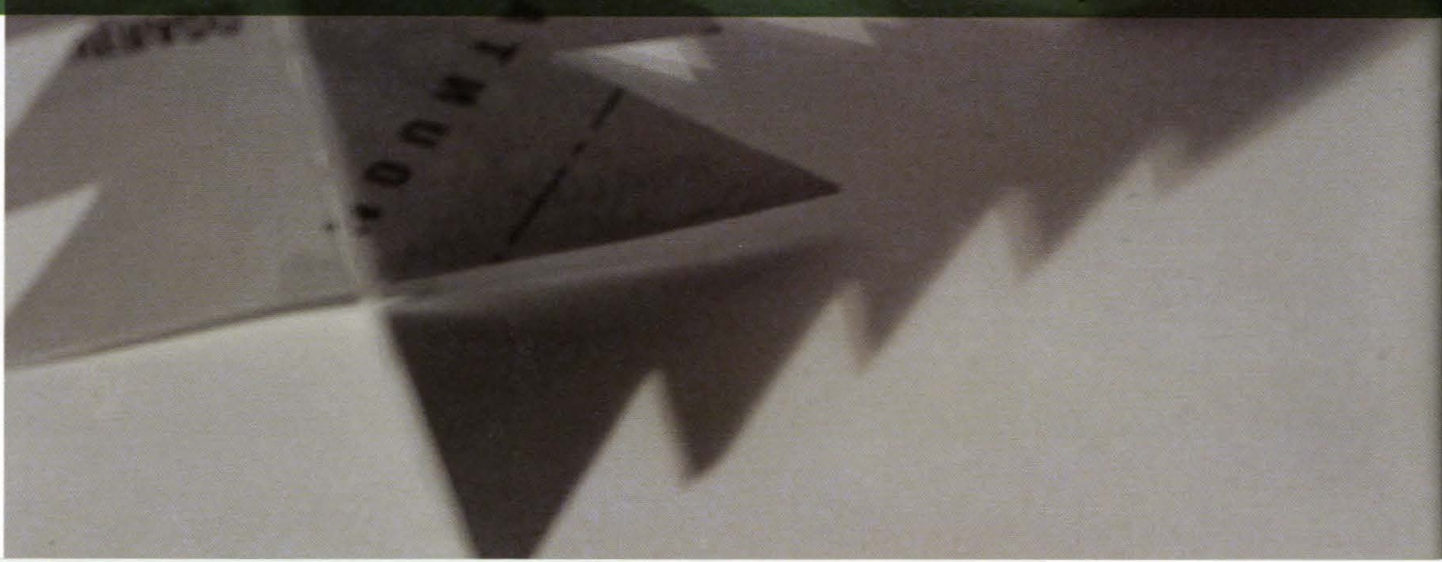

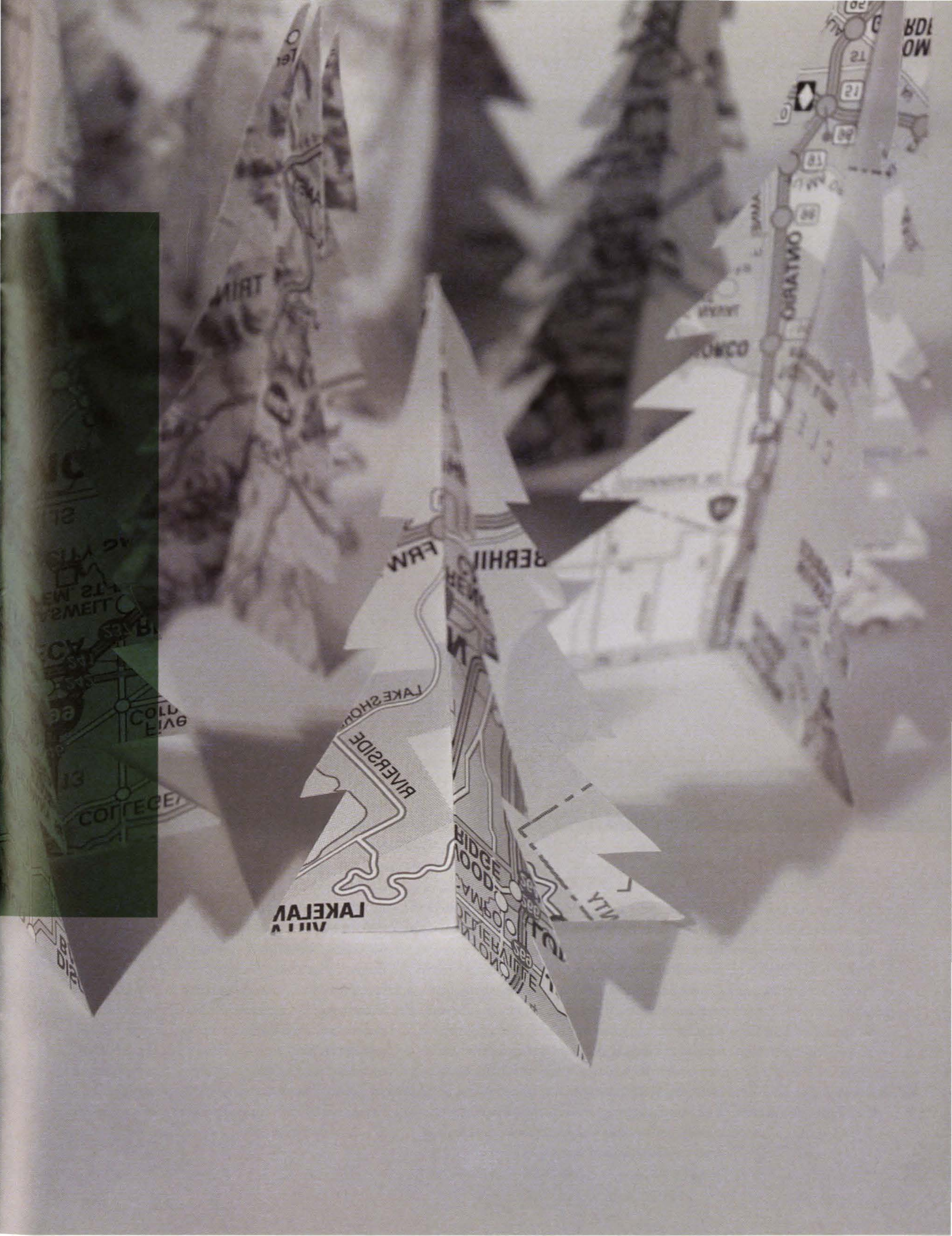
RIVERSIDE

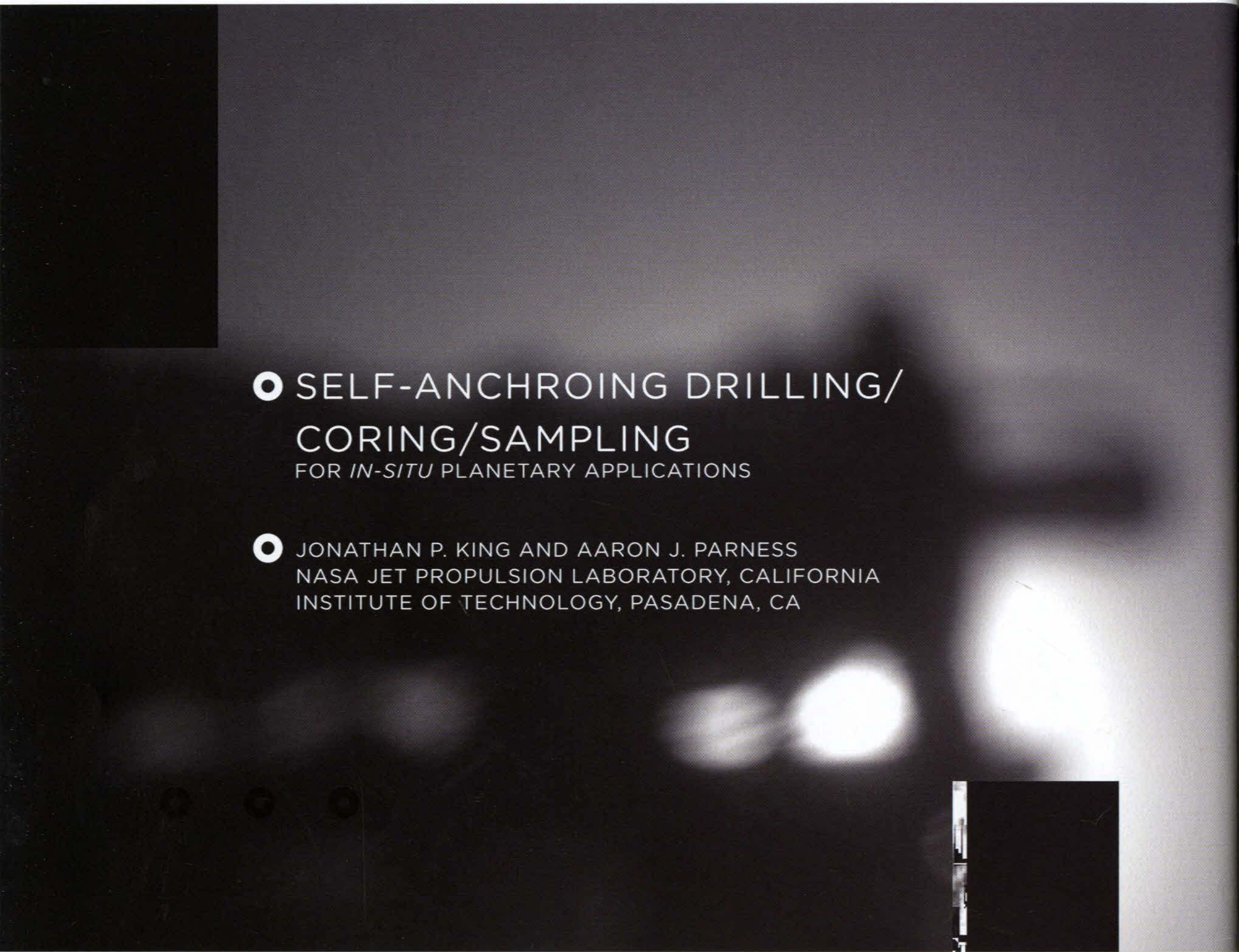

SELF-ANCHROING DRILLING/ CORING/SAMPLING

FOR *IN-SITU* PLANETARY APPLICATIONS

JONATHAN P. KING AND AARON J. PARNESS
NASA JET PROPULSION LABORATORY, CALIFORNIA INSTITUTE OF TECHNOLOGY, PASADENA, CA

ABSTRACT

The objective of future NASA exploration missions is *insitu* sampling and analysis of various astronomical bodies in the solar system and return of samples to Earth for further study. Conventional drills require a relatively high axial preload, or weight-on-bit, which limits their use in microgravity and on inverted surfaces. To resist these large reaction forces during drilling, an anchoring mechanism that effectively clings to rough and rocky surfaces has been adapted for use with a coring drill. The system consists of a compact rotarypercussive drill with a custom coring bit, a linear translation mechanism with preloaded compression springs that maintain weightonbit, and a compliant anchoring mechanism that employs an omnidirectional array of microspines that anchor to a surface. Fabrication of a prototype based on this design was accomplished through a variety of manufacturing processes including rapid prototyping techniques such as shape deposition manufacturing and selective laser sintering. Successful demonstrations of the system supporting itself while working against gravity in an inverted position provide convincing proof of concept for the use of microspine anchors as load bearing structures during insitu sample acquisition in microgravity and/or on inverted surfaces.

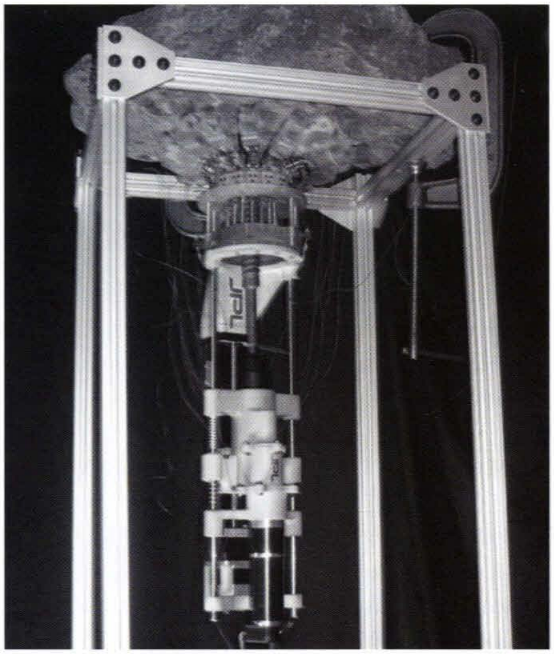

Figure 1: Inverted Drill Test; System anchored to inverted surface, drill working against gravity (Harder than Zero-G).

I. INTRODUCTION

The objective of future NASA exploration missions is insitu sampling and analysis of various astronomical bodies in the solar system including, but not limited to, Mars, Europa, Titan, comets and asteroids.

Such samples could provide insights on the formation of the solar system and perhaps even the origins of life on Earth. If such missions are to occur safely and successfully, conventional sampling methods must be adapted to meet the additional challenges posed by operating on these bodies.

Operations occurring on a near-Earth asteroid will prove difficult due to differences in mass and hence gravitational effects between asteroids and other lunar or planetary bodies. Asteroids generally have microgravity conditions; microgravity conditions are characteristically described as having a weak gravitational field due to low mass. In order to get data from smaller bodies like asteroids without flying off into space due to the asteroid's significantly weaker gravitational field, robots and even astronauts will need more efficient methods of anchoring themselves to the surface. Working toward such goals, JPL is investing in a technology known as microspine anchoring.

Anchoring technology has many applications currently being researched, several that extend beyond microgravity, including static support anchors to act as endeffectors for limbed robots. Thanks to these anchoring technologies, exploration of steep cliffs and even inverted surfaces such as those found in lava tubes on Mars may be possible. For sample acquisition, scientists have focused on improving drilling techniques and reducing the amount of force required to penetrate a surface, known as weight-on-bit (WOB). Previously, drilling and other sampling methods have transmitted their reaction forces to a robot or structure through robotic arms or booms. Instead, my research focuses on adapting microspine anchoring technology so it can act as the load bearing mechanism for insitu drilling and sampling applications. By decoupling the robot from reaction forces caused by drilling, the robot no longer needs to compensate for them through an overly complex initial design. The result of my research is a prototype system capable of drilling core samples in natural rock independent of orientation and gravitational field, the highlight case was anchoring to an inverted surface and proceeding to drill against gravity, a harder than zero-gravity test setting. Successful trials provided proof of concept (that it works for small scale terrestrial tests) for the anchor's use in microgravity drilling; Test setup shown in Figure 1.

II. OBJECTIVES

Research goals this summer at JPL were to demonstrate proof of concept for a sample acquisition system supported by a compliant microspine anchor. Before succeeding in the research objective, we needed to modify a rotary percussive drill to minimize size and fit within the system, create a mechanism that translates the drill into the surface while maintaining WOB, and design an assembled system able to mount to a surface.

III. MANUFACTURE & ANCHOR ASSEMBLY

A. Construction of the Drill

The first item to address concerning the drill is the choice of a 36 V rotary percussive rather than a traditional rotary drill. Traditional rotary drilling is an abrasive process in which a rotating bit grinds away at the surface, this technique is slow and consumes a lot of energy in addition to transmitting a larger amount of torque to the support structure. Rotary percussive drilling however is faster, more energy efficient, transmits less torque to the support and has a longer tool life. After building a mockup demonstrating the design concept, the commercial drill was disassembled and the new housing was designed with CAD to contain the drilling mechanisms as well as the new drive motor; before and after photos of drill shown in Figure 2.

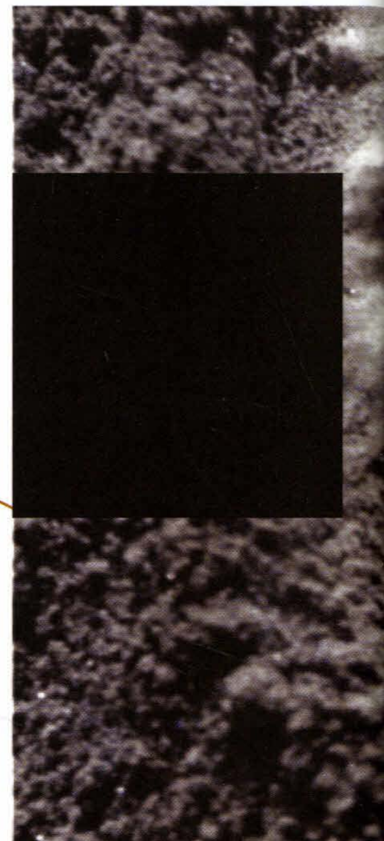

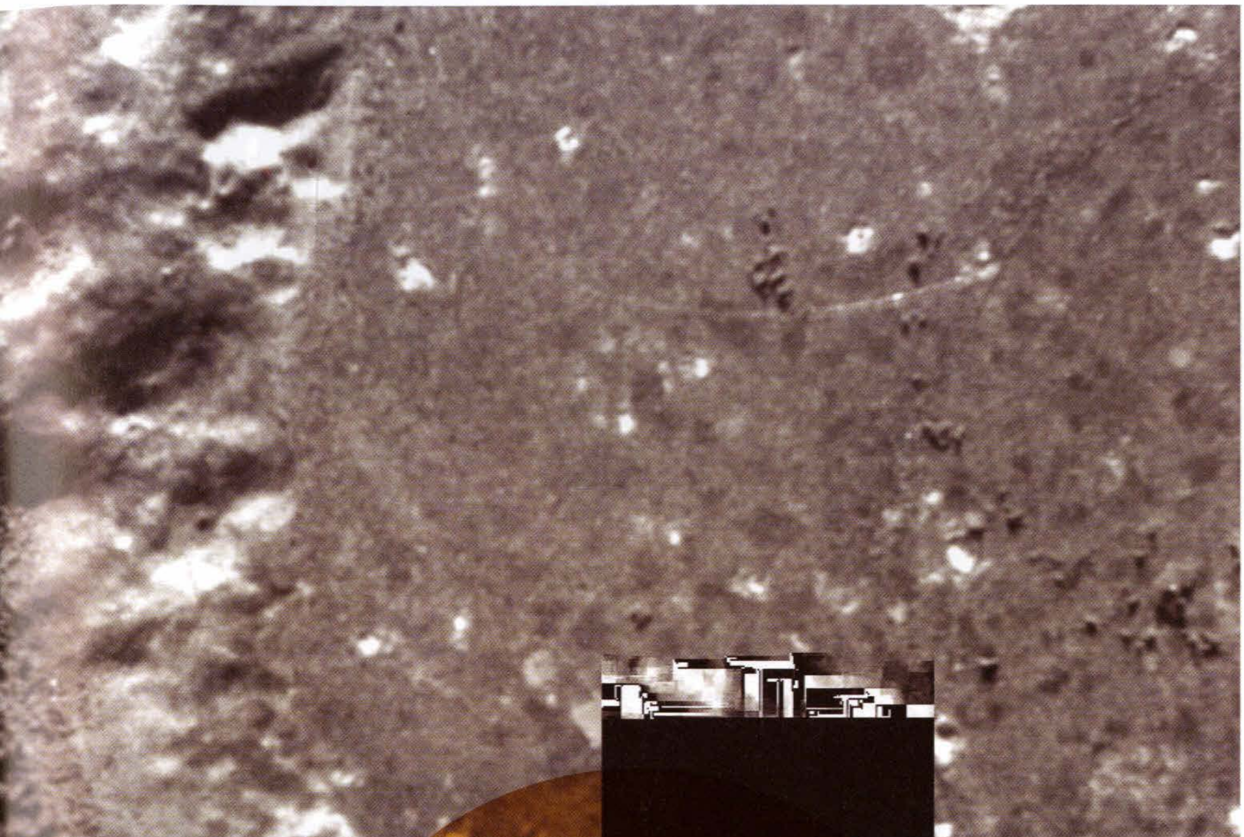

CONVENTIONAL DRILLS REQUIRE A RELATIVELY HIGH AXIAL PRELOAD, OR WEIGHT-ON-BIT, WHICH LIMITS THEIR USE IN MICROGRAVITY AND ON INVERTED SURFACES.

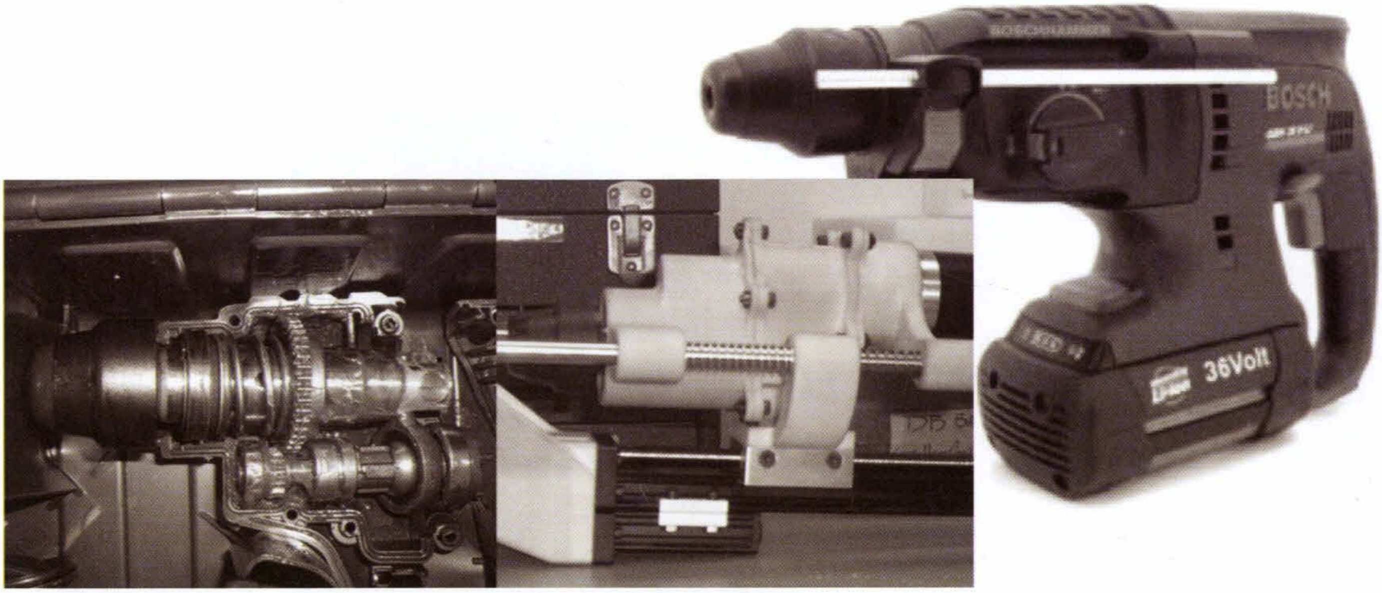

Figure 2: (*left*) Extracted interior mechanism. (*middle*) Redesigned housing, preloaded compression springs and linear translation mechanism supplying WOB. (*right*) Commercial drill.

B. Weight-On-Bit and Translation

The most fundamental parameter to consider in automated drill applications is known as weight-on-bit or WOB. This is the amount of force required about the drilling axis to penetrate the surface and carry out drilling. The WOB for our drill tests was estimated including compensation for the drill mass, 1.78 kg, to be about 60 N when drilling into vesicular basalt rock in an inverted orientation. The WOB was supplied by preloaded compression springs that could supply up to 80 N of force when fully compressed in parallel.

During drilling, it is necessary to incorporate guide rails on the system so that the drilling axis remains fixed and also to prevent the springs from buckling. Fixing the drill axis results in some torque being transmitted to the anchor as well as bending moments depending on the orientation of the system. To compensate for torque and bending as well as potential errors in machining, six self-aligning linear ball bearings were used, each capable of correcting for 1.5° of axial misalignment. The linear bearings were press fit into their custom designed housings and then held in place with retaining rings. Finally, a custom coring bit with carbide tips was purchased, specifically designed to core through extremely hard rock such as vesicular basalt; Final system shown in Figure 3.

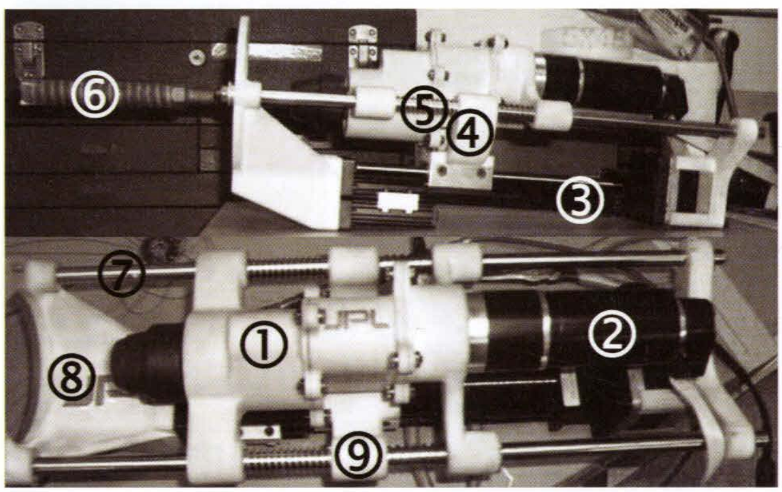

Figure 3: Top and side view of assembled drill showing housing (1); drive motor (2); linear translation mechanism (3); slide carriage (4); compression springs x4 (5); bit (6); guide rails x2 (7); mounting plate (8); and housed linear bearings x6 (9)

IV. METHODOLOGY

A. System Design

Computer-aided-design, CAD, software greatly helped the design process. Using CAD software allowed for the creation of a digital prototype in only 5 weeks; CAD render shown in Figure 4.

B. Testing Method

The test method chosen for the drill system, shown in Figure 1, is known as the Inverted Drill Test. This orientation provided confirmation of the anchors ability to support a static load while upside down or inverted, as well as its ability to support any forces reacted from drilling operations carried out on the rock surface.

Testing was performed by controlling the drilling via a power supply that regulated the voltage, kept constant at 24V, and the current, varied between 1.5A and 7A. The test was carried out on several rock samples with mostly positive results; discussed in the results section.

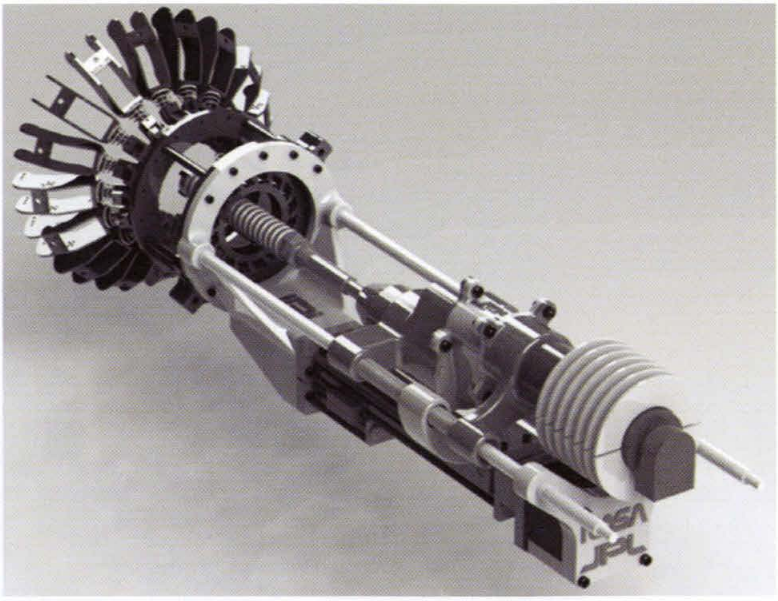

Figure 4: CAD model of final drill design.

V. RESULTS

A. Test Results

Testing on multiple samples yielded mostly positive results. The anchor was able to establish grip on every rock tested, and was able to maintain grip through drill preloading on every rock tested. The system went on to successfully drill into all but one of the rocks chosen, albeit after the anchor had been damaged during testing procedures unrelated to this project. The most successful test was carried out on a sample of red vesicular basalt; the system achieved a drill rate of 1.5 inches per minute and a drill depth of 4 inches, the maximum allowed by the coring bit. After drilling, a core sample was acquired from the coring bit after disengaging the drill system.

B. Implications of Results

Results show that this system concept works for the application of selfsupported drilling using microspine anchors. Additionally, these results show that the anchor is capable of supporting loads independent of orientation, implying that that the drill may be useful in a variety of applications involving remote instrument placement or loading support. By testing the system in an inverted orientation, the system was working against Earth gravity, or "harder than zero gravity", therefore the results indicate the system would work just as well if not better in a microgravity environment. By creating a selfsupporting system that works independent of orientation or gravity, and is not positionally constrained by a robotic arm, we have created the potential for a wide range of deployable, selfcontained remotely operated robots capable of anything from remote observation to load support to sample acquisition.

Some of the more immediate applications of such systems include insitu sample acquisition in microgravity, challenging terrain (i.e. steep cliffs or underwater) and hard to access terrain (i.e. lava tube ceilings). This technology may also have applications for improved operations found throughout commercial and industrial drilling conventions.

VI. CONCLUSION

An omnidirectional anchoring mechanism adapted for use in an insitu sample acquisition system was presented that can withstand over 100 N of force and acquire a 4 inch core sample. A test setup was chosen that provided proof of concept for the systems use in microgravity. Future development of this technology will provide several of the capabilities needed to carry out future NASA missions.

ACKNOLWLEDGEMENTS

Jonathan P. King would like to acknowledge Aaron Parness, Matt Frost, and Brett Kennedy for their assistance, advice, mentorship, and continued support throughout his research experience at the Jet Propulsion Laboratory. In addition he would like to thank the California Institute of Technology, SURF, and all of the staff involved in the aforementioned entities as well as the JPL education office for making this opportunity possible. This research was conducted at the National Aeronautics and Space Administration Jet Propulsion Laboratory, California Institute of Technology, and was sponsored by the Summer Undergraduate Research Fellowship program through the California Institute of Technology.

FURTHER READING

Parness, A., "Anchoring Foot Mechanisms for Sampling and Mobility in Microgravity," IEEE International Conference on Robotics and Automation, NASA Jet Propulsion Laboratory, California Institute of Technology, Pasadena, CA, 2011.

Okon, A., "Mars Science Laboratory Drill," Proceedings of the 40th Aerospace Mechanisms Symposium, May 2010.

NAVSEA

NAVAL SEA SYSTEMS COMMAND

EXTRAORDINARY CIVILIAN CAREERS, UNIQUE POSSIBILITIES

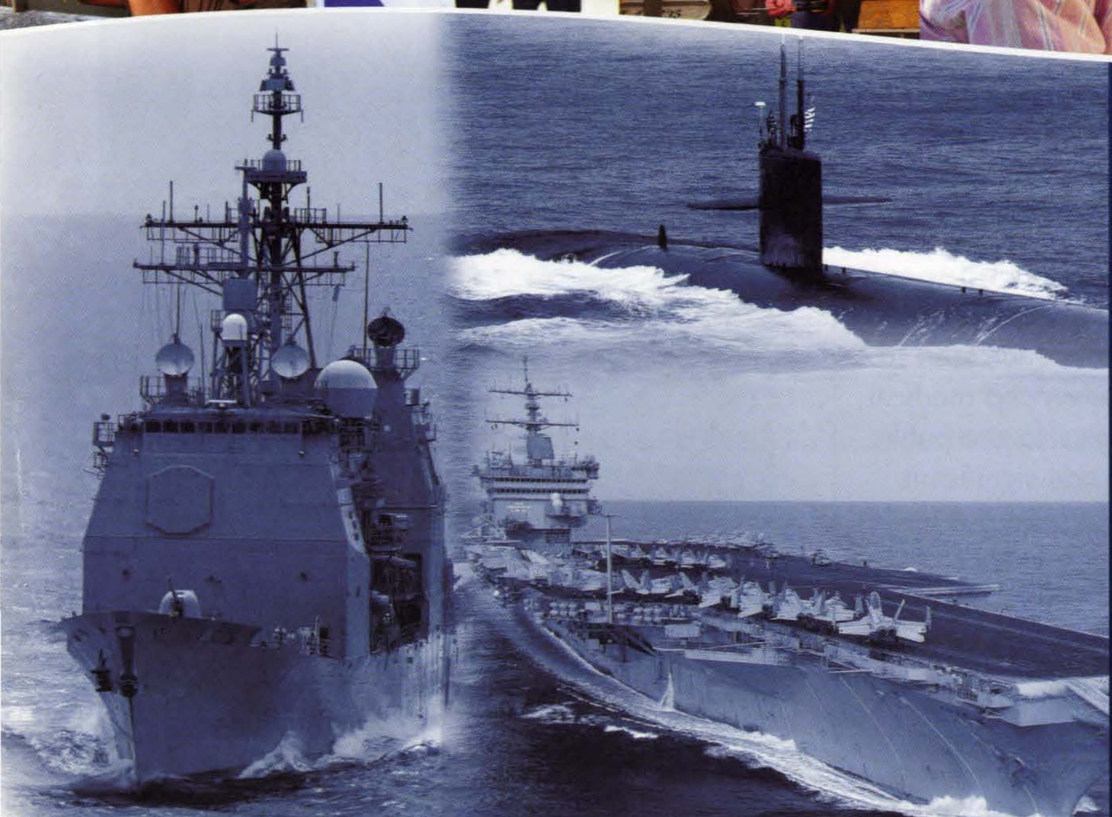

Imagine tomorrow...

Then come and create it as a civilian engineer, scientist, accountant, or contract administrator within the Naval Sea Systems Command.

www.navsea.navy.mil

U.S. Citizenship Required